Synthesis, Characterization, and Equilibrium and Kinetic Studies of an Unusual Cobalt to Carbon Alkyl Bond Rearrangement in the Coenzyme B_{12} Model Complex $C_6H_5CH_2Co^{III}[(DO)(DOH)_{pn}]I$: A Carbon-Benzyl Bond Dissociation Energy of 23 kcal/mol

by

Brian E. Daikh

A Thesis

Presented to the Department of Chemistry
and the Honors College of the University of Oregon
in partial fulfillment of the requirements
for the degree of Bachelor of Arts

June 1990

Approved [redacted]

Dr. Richard G. Finke

ACKNOWLEDGMENTS

I wish to express my gratitude to Dr. Richard Finke for his patience and support throughout the duration of this endeavor. I thank the American public for their support through NIH grant #DK 26214 to Dr. Finke.

I thank Dr. Tim Weakley for his work on the x-ray crystal structure analysis and Chuck Klopfenstein for his 500 MHz NMR work.

I also wish to thank Dr. Bruce Martin for many hours of support and constructive criticism. Thanks also to the rest of the Finke group for their support; David, Cheryl, Yun, Noritaka, Matthias, Yin, and Paul.

Finally, I wish to thank my family who have always been available for advice and financial support.

LIST OF FIGURES

LIST OF SCHEMES AND TABLES

BACKGROUND

Coenzyme B_{12}, 5'-deoxyadenosylcobalamin, a derivative of vitamin B_{12}, is a molecule of particular interest to both chemists and biochemists. Although it is a very important molecule to several familiar biochemical reactions, we, as of yet, do not fully understand the mechanism through which B_{12} functions. B_{12} works with a number of different enzymes to catalyze at least twelve chemical reactions of two principle types: organic skeletal rearrangements and biological methylations. Enzymes, using an analogy, are the machinery in the factory (our bodies) which produce all the essential chemical building blocks which make up our body and keep us alive. They also break down or modify chemical building blocks obtained by food consumption. Enzymes are catalysts, that is, they are regenerated at the end of a chemical reaction so they can catalyze the same reaction again. One enzyme can catalyze a reaction thousands of times before it "dies". However, because enzymes "die", they must be made constantly. Though it is not understood well at all, it is thought that the process of aging may in part be linked to: the body's ability to produce enough enzymes, defects in the enzymes themselves, especially older enzymes, or a combination of the above.

B_{12} is unique in that it is the only biological molecule known to contain cobalt. The key structural features of the coenzyme are (Figure 1): the cobalt atom, which is surrounded by four nitrogens of the corrin ring, the base (α-ribazole), which is in the axial base

Figure 1

Coenzyme B_{12}

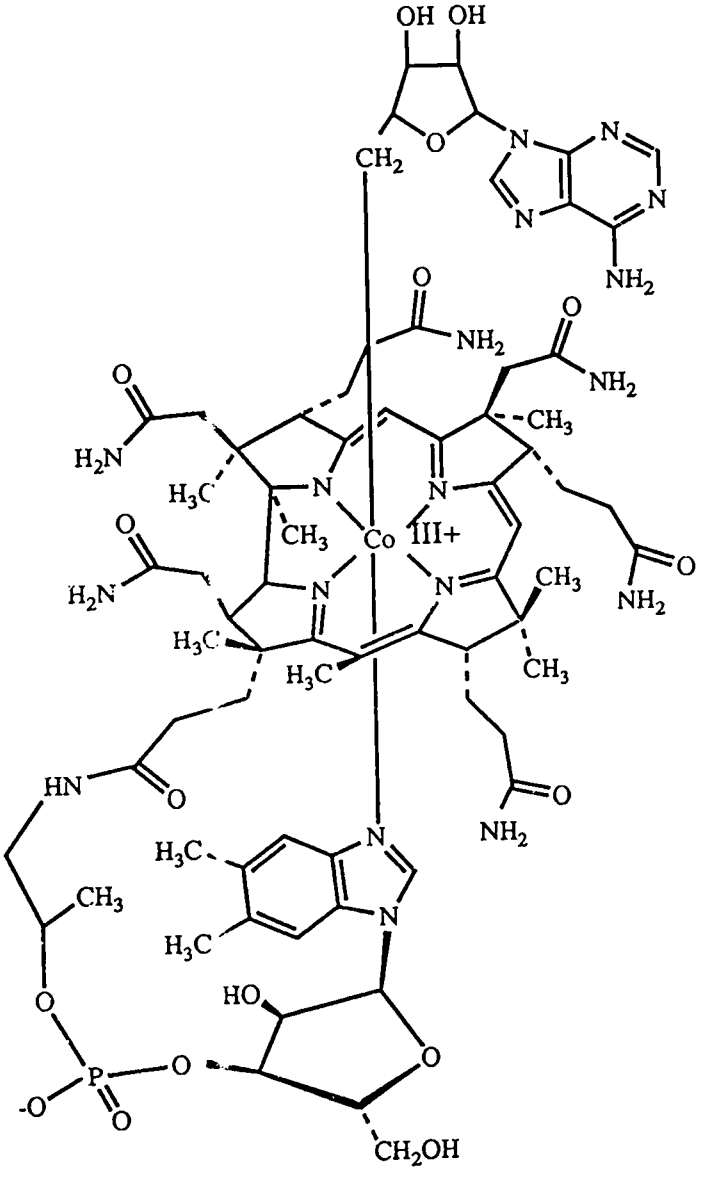

position; and the adenosine nucleoside, which is connected to the molecule via a cobalt-carbon bond. The most unusual feature of the molecule is this cobalt-carbon bond, which is not found in any other naturally occurring molecule. It is the homolysis* of this bond that is suspected to be the coenzyme's main function. It is not yet known whether or not the cobalt participates in any subsequent part of these chemical reactions.

One of the key goals of Richard Finke's research group is to determine the mechanism of coenzyme B_{12}-dependent rearrangements. Before the group began to study the coenzyme itself, however, model compounds were used to study the cobalt-carbon bond homolysis. It was thought at the time that because of its size and complexity, B_{12} itself would be too difficult to study. This, in part, proved correct, but B_{12} itself is now used.

The principal model compound developed and studied by the Finke group was trans-benzyliodo(trimethylenedinitrilo)-bis(3-oximato-2-pentanone)cobalt(III), hereafter known as $C_6H_5CH_2Co^{III}[(DO)(DOH)_{pn}]I$, compound 1 (Figure 2). This molecule was chosen because both its structure and presumably the chemistry of its cobalt-carbon bond are similar to B_{12}, though it is a much simpler molecule. It contains a cobalt atom coordinated between four nitrogens analogous to the corrin ring in B_{12}, but the substituents of the ring itself are much simpler than that of B_{12}. A benzyl group and an iodine atom occupy the axial positions. Another key difference is that B_{12} is a zwitterion (a molecule with a positive charge in one place and a negative charge in a

---

*See glossary for a list of terms and their definitions.

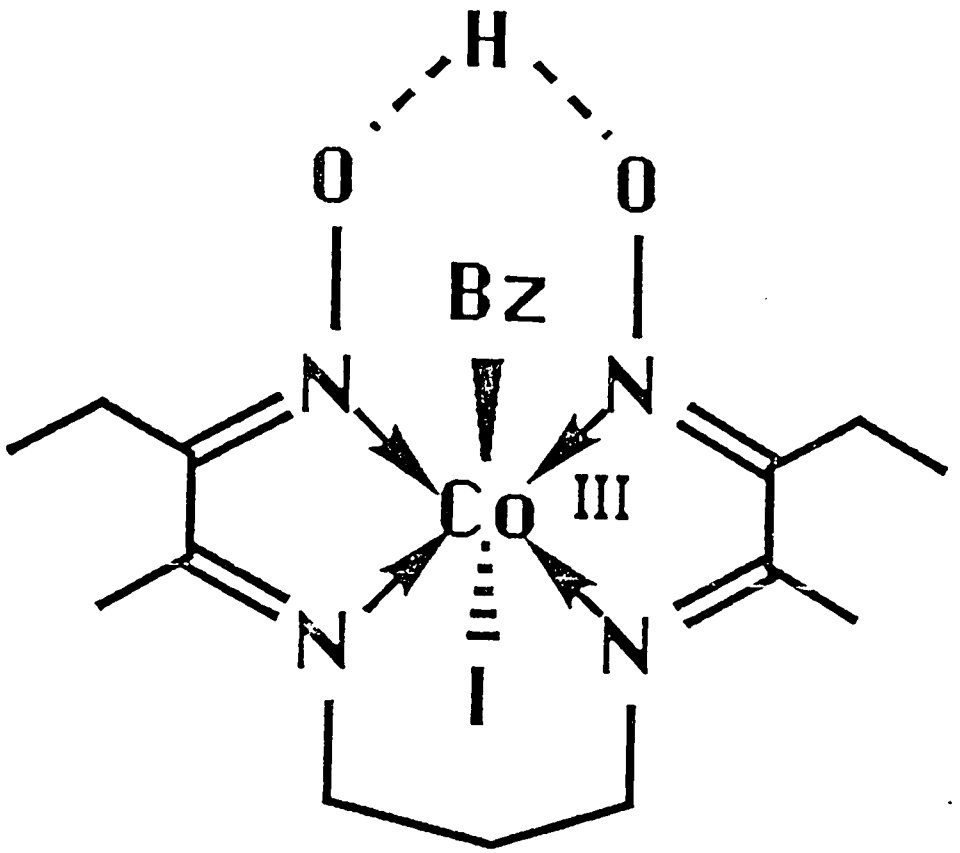

$C_6H_5CH_2Co^{III}[(DO)(DOH)_{pn}]I$, 1

second part of the molecule, but is overall neutral), while the model is not.

The research contained in this thesis involves the chemistry of this model compound, specifically the study of a new molecule made as a result of 1 rearranging when exposed to heat or light. This chemistry is important to study because it is a little studied type of reaction and could, for example, provide information about catalyst degradation pathways. The goal of this research is to characterize fully the rearrangement product, to study the kinetics of the reaction which forms it, and ultimately, to propose a mechanism for its formation.

It is important to learn as much as possible about the chemistry of this new molecule for several reasons. First, since no others have been reported, this molecule is presumably the first to demonstrate this particular type of rearrangement. Consequently, this knowledge would be very interesting to chemists who study organometallic compounds (organic molecules which contain metal atoms), especially those who study the nature of the metal-carbon bond. Second, reversible migrations such as this one have not been well documented and are largely unknown. This rearrangement may be important to metallofactor catalyst degradation (eg. B_{12}). Third, the rearrangement product may be important to how B_{12} works. Restated, it may be similar in structure to what B_{12} looks like while B_{12} is actually catalyzing a reaction (often some higher energy species which cannot be put in a bottle or examined directly does the actual catalysis). Fourth, 1 is just one of many similar molecules which have been synthesized to study B_{12}. However, other than their obvious similarities to B_{12}, very little is known about their chemistry, stability and reactivity. Understanding the structure and formation of

this rearrangement product will provide valuable information about these molecules which have not previously been studied in great detail. Fifth, though these molecules do not, as of yet, have any direct usefulness other than their use in studying B_{12} (probably because not enough of their chemistry is known) it is of intrinsic value to the continued accumulation of chemical knowledge that we learn as much as possible about them. Finally, and perhaps most importantly, because we do not understand these molecules, we should study them, for experience teaches that putting our effort into things that we understand the least yields the most important results.

INTRODUCTION

As part of cobalt-carbon thermolysis bond dissociation energy studies[1] reported previously, an unusual product was formed in the absence of the free radical trap TEMPO. A number of confusing observations were made which caused us to pursue this product in hopes of better understanding the chemistry involved: The product was red in color (similar to Co^{II}•) with λ_{max} = 525 nm (Co^{II}• = 522 nm), yet the product was diamagnetic by NMR, unlike Co^{II}• which is paramagnetic; no (<5%) bibenzyl, a well-known radical termination product, was observed; the product contained low symmetry by ^1H NMR in contrast to the very symmetrical parent compound; the benzyl group was still present in the molecule however, but not on cobalt (i.e. the molecule is a structural isomer of the starting material); the reaction appeared to be related to several reports of rearrangements in similar porphyrin, cobaloxime, and salen ring systems (most of which are structurally ill-defined).

Herein is reported the synthesis, characterization, and kinetic studies of this product, (SP-5-15)-[2-[[3-[[2-(hydroxyamino)-1-methyl-2-(phenylmethyl)butylidene]-amino]propyl]imino]-3-pentanone oximato(2-)-N,N',N''N''']iodocobalt, 2. The results described report an unprecedented cobalt-carbon to macrocycle carbon reversible benzyl migration, including characterization of the product by x-ray crystallography, and rate and equilibrium constants for both the forward and reverse migration reactions.

Photolysis of $C_6H_5CH_2Co^{(III)}[(DO)(DOH)_{pn}]I$, 1, in the absence of TEMPO radical trap gave an unusual product 2 (Scheme 1). NMR showed that the bridging hydroxylic proton of 1 was still present in 2, but had shifted from δ 20.24 to δ 17.47 (in d_6-benzene). Similarly, the benzyl peaks of 1 were still present, but had changed in number from three to two in 2. This evidence suggested that the macrocycle was still intact, but that the benzyl group previously attached to cobalt had migrated to another position within the molecule, a phenomenon previously documented especially in porphyrin (but not in the present) systems.

The crystal structure of 2 provided the unprecedented result that the benzyl group had migrated, not to a ring nitrogen as suggested by the literature, but to a ring carbon adjacent to nitrogen, trans to the iodine atom. The elemental analysis and mass spectrum of 2 were consistent with the crystal structure; together the results require that 2 is a more stable isomer of 1.

Photolysis of 1 at ambient temperature quantitatively yielded 2 (100 ± 5%) both by ^1H NMR and by visible spectroscopy. Photolysis of 1 at 69°C also quantitatively yielded 2.

Thermolysis of 1 in the absence of TEMPO trap did not yield pure 2, but rather a mixture of 1 and 2. The ratio of the two species in the mixture was constant over a 26°C temperature range (69-85°C), 40 ± 2% 1 and 60 ± 2% 2. The same mixture was obtained starting with either 1 or 2, which indicates that the migration is reversible. The total sum of the two hydroxylic protons remained constant throughout the reaction and there was no sign of bibenzyl or Co^{II}• by ^1H NMR, suggesting that the reaction proceeds cleanly. Thermolysis of either 1 or 2 at visible

Scheme 1

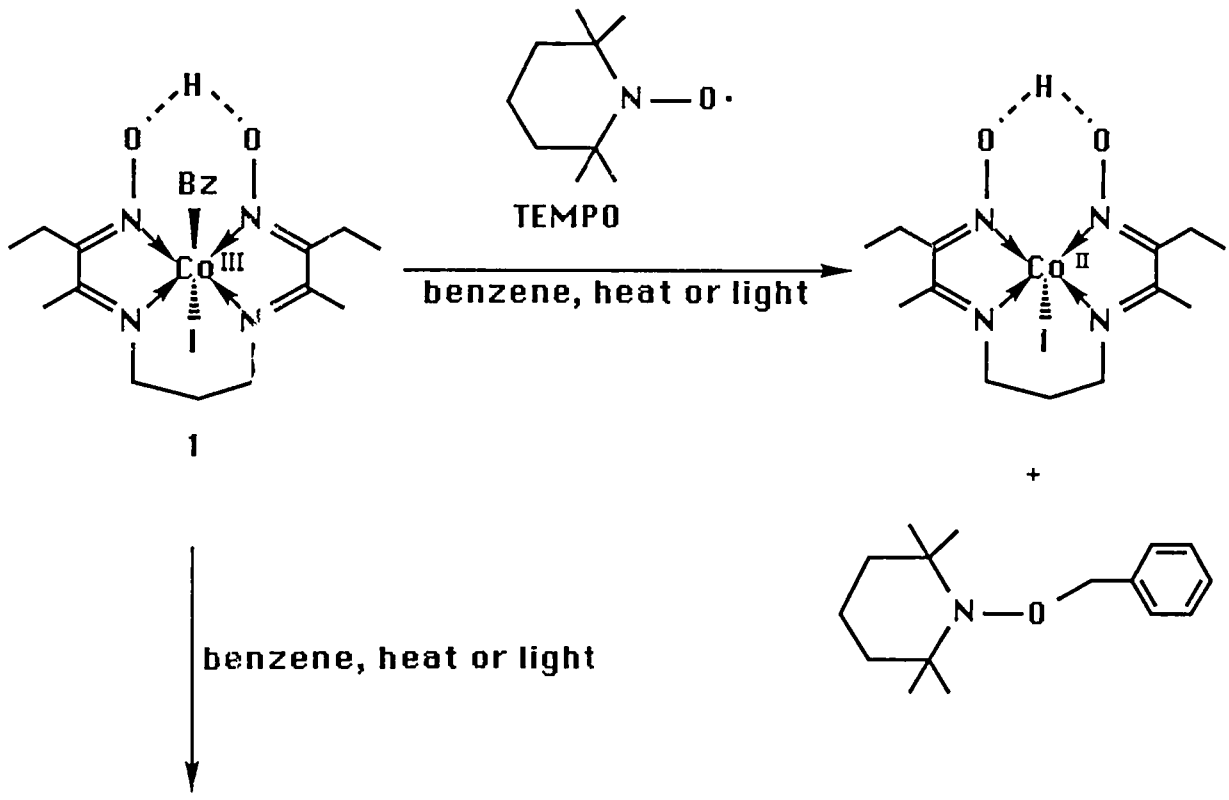

1

2

spectroscopy concentrations (ca. 1×10^{-4} M) also proceeds cleanly. The final spectrum matched that of a weighted average spectrum of 40% 1, 60% 2 (±5% machine uncertainty).

This temperature-independent 40/60 ratio implies that $K_{eq69°} = 1.5 \pm 0.1$, which in turn implies that $\Delta G^{o}_{69°} = -0.28 \pm 0.02$ kcal/mol, $\Delta H^{o} = 0.00 \pm 0.02$ kcal/mol, and $\Delta S^{o} = 0.82 \pm 0.06$ cal/mol•K. Exponential fitting of ^{1}H NMR data indicated first-order kinetics with $k_{obs} = 3.6 \pm 0.7 \times 10^{-5} sec^{-1}M^{-1}$. This value and K_{eq} imply $k_1 = 2.2 \pm 0.9 \times 10^{-5} sec^{-1}M^{-1}$ and $k_{-1} = 1.4 \pm 0.3 \times 10^{-5}$ $sec^{-1}M^{-1}$.

Thermolysis of 2 with TEMPO quantitatively yielded $Co^{(II)}$ and benzylTEMPO (96 ± 6%) by gas chromatography. An Arrhenius plot of ln *k* vs. 1/T for four temperatures over a 30°C temperature range gave a linear plot with $\Delta H^{\ddagger} = 25 \pm 1$ kcal/mol, $\Delta S^{\ddagger} = 8 \pm 3$ e.u., and $\Delta G_{25°}^{\ddagger} = 27 \pm 1$ kcal/mol. The rate constant for this trapping reaction was 1.6×10^{-5} sec^{-1} at 69°C, 31x smaller than the rate constant for the reaction of 1 and TEMPO at 69°C (5.0×10^{-4} sec^{-1}).

LITERATURE BACKGROUND

There are a number of papers in the literature which demonstrate alkyl migrations as well as migrations of other groups from metal centers to equatorial ligands in some systems. However, many of these papers may be of little relevance due to the fact that they propose migrations to nitrogen (mostly without structural evidence), while our crystal structure of 2 demonstrates an unprecedented migration to carbon.

Papers by Gaudemer[2], Balch[3], and Mansuy[4-6] all remain relevant, however, as they all demonstrate reversibility in their ligand migrations. Our system consisting of 1 and 2 has also proven to be reversible.

Using alkylcobaloximes, Gaudemer studied electrolytic reductions of organic compounds involving alkyl-cobalt intermediates. The cleavage of the cobalt-carbon bond during reduction of the alkyl-cobalt compounds was confirmed by cyclic voltammetry. With some optically active cobalt compounds, complete retention of configuration was observed. To account for this result, reversible trapping of the alkyl groups by the equatorial ligand was proposed. Gaudemer postulates that the alkyl group is transferred to an "appropriate position" on the equatorial ligand by an undefined mechanism. He suggests nitrogen, but no structural evidence is given. Note that our crystal structure data now suggest, as the better precedented possibility, migration to carbon.

Mansuy found evidence for reversible metal-to-nitrogen migration of alkyl, aryl, vinyl, and vinylidene groups, and O-C-C moieties in iron porphyrins. He provides structural evidence for some of these compounds.

Balch also demonstrates reversible migration of axial carbenes into the Fe-N bond of porphyrin models.

One possible mechanism for the formation of 2 finds precedence in work by Espenson.[7] Espenson studied alkylaquocobaloximes and proposed that the radical addition takes place at the nitrogen end of the N-C bond on the $(dmgH)_2$ pseudomacrocycle, cis to the Co-C bond, followed by the reductive elimination of RR'. However, this mechanism predicts the opposite of our inability to find bibenzyl.

Kochi[8] has reported a short chain-length radical-chain reaction where a key new feature is the apparent S_H2 reaction, not at carbon, but overall at cobalt and apparently on the six-coordinate complex. Their results seem to require some intermediate and Kochi writes an N-R bound alkyl as the intermediate, but again our crystal structure suggests a C-R bound alkyl as the better precedented possibility. Since Kochi has reported such an intermediate, we must consider such a radical-chain reaction as a possible mechanism for the formation of 2. Richard Finke[9] has worked out the kinetics for a Kochi-type mechanism for the formation of 2 (an addition-elimination, net S_H2 propagation) and has found the expected rate to be second order in 1. This is inconsistent with the observed kinetics which are first order in 1 and hence, though Kochi's intermediate may be like 2 structurally, this mechanism can be ruled out. Note that Espenson's mechanism can also be ruled out as a possibility as it also demands second-order kinetics in 1 or 2.

RESULTS

Product Studies

X-ray crystal structure of 2 (Figure 3)[10]:

The benzyl group has migrated from the sixth coordination site on Co(1), *trans* to I(1), to the atom C(7) adjacent to the oxime nitrogen atom N(4). It remains on the side of the ring system remote from I(1). The ring system can be considered in three parts.

(i) The chelate ring Co(1)-N(1)-C(1)-C(2)-N(2) is planar to within 0.08 Å. The Co(1)-N(1) (oxime) and Co(1)-N(2) (imine) bond lengths (Appendix 2, Table A3) are respectively at the lower and upper limits of the ranges observed in related complexes. Other dimensions are normal.

(ii) The six-membered ring Co(1)-N(2)-C(3)-C(4)-C(5)-N(3) is puckered, as expected. It shows no disorder as the central methylene atom C(4) occupies a single site on the side of the mean plane of the other five ring atoms remote from I(1).

(iii) The ring Co(1)-N(3)-C(6)-C(7)-N(4) is planar to within 0.035 Å but its mean plane is inclined at 21° to the mean plane of the other five-membered ring. The change in bond hybridization at C(7) from sp^2 to sp^3, accompanying the benzyl group migration, has allowed N(3) to remain almost coplanar with Co(1), N(1), and N(2), but has displaced N(4) 0.69 Å from the Co(1),N(1,2,3) mean plane away from I(1). Also *both* the N(4)-Co(1) and the N(4)-O(2) bond lengths [1.78(1), 1.28(1) Å]

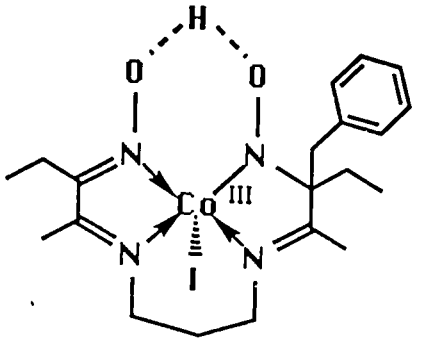

2

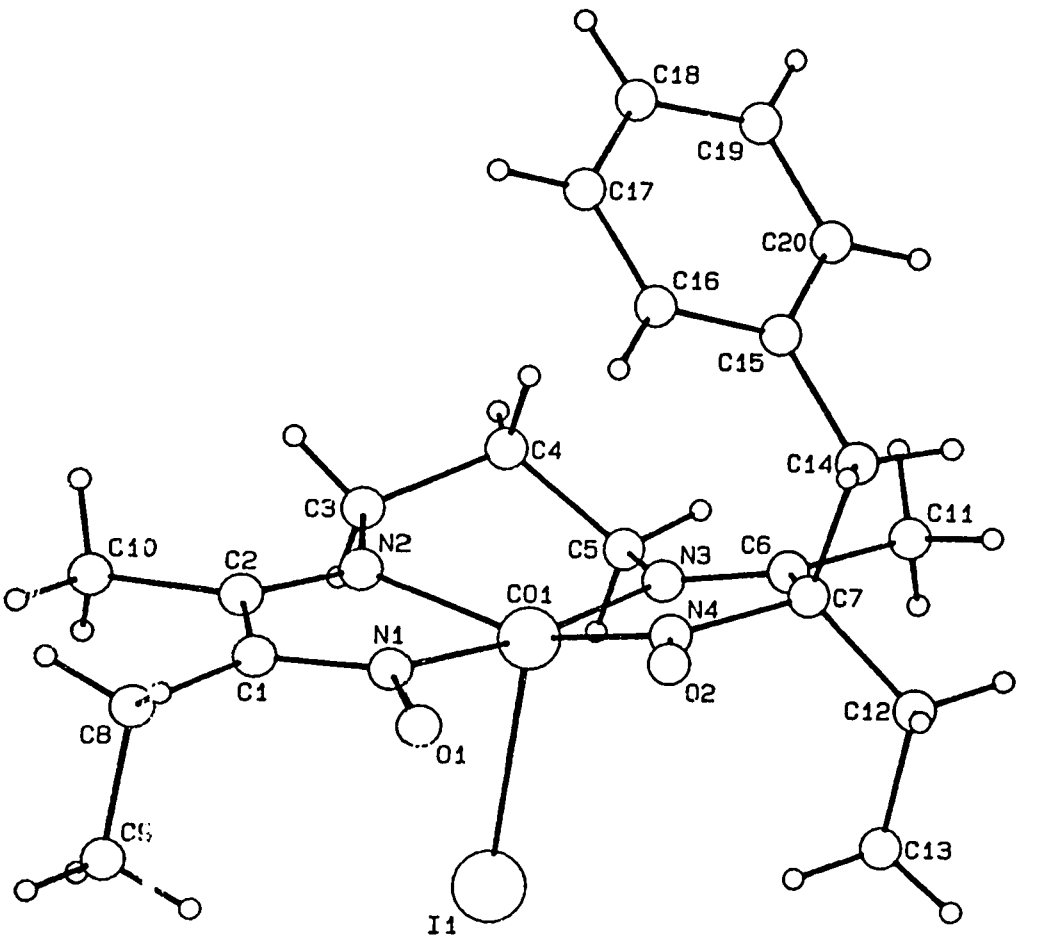

Figure 3: X-ray crystal structure of (SP-5-15)-[2-[[3-[[2-(hydroxyamino)-1-methyl-2-(phenylmethyl)butylidene]-amino]propyl]imino]-3-pentanone oximato(2-)-N,N',N'',N''']iodocobalt, 2.

are significantly shorter than their 'normal' counterparts N(1)-Co(1) and N(1)-O(1) [1.86, 1.38(1) Å].

The O(1)..O(2) distance, 2.47(1) Å, is at the upper end of the range of values found in related Co complexes. The hydrogen atom of the probable intramolecular hydrogen bond could not be located. The phenyl ring is placed so as to hinder access to the vacant coordination site on Co(1), but the shortest C(phenyl)-Co distance [C(16), 3.79(2) Å] is far too long for significant bonding. There are no short intermolecular contacts. See Appendix 2 for supplemental x-ray crystallographic data.

Photolysis and Thermolysis Reactions

The photolysis of 1 at UV/vis concentration was complete within ca. twenty minutes by visible spectroscopy. The λ_{max} of 1 at 417 nm decreased to a minimum with time, while the λ_{max} of 2 at 525 nm grew in with time. The reaction proceeded with a clean isosbestic point at 466 nm (Figure 4). This result is consistent with the NMR data an indicates that the formation of 2 from 1 by photolysis is a clean reaction (ie. there are no other products or intermediates formed).

A small peak in the ^{1}H NMR spectrum of 2 has consistently appeared at δ 17.37, adjacent to the bridging hydroxylic proton peak at δ 17.47. Integration of the two peaks yielded a ratio of 91 ± 2%/9 ± 2% respectively (Figure 5). In a control experiment designed to test whether or not the crystalline form of 2 was the predominant (91%) or minor (9%) structural form, 500 MHz proton NMR of crystals of 2 revealed the same two peaks in the same ratio. Because the additional peak is so far downfield and is so close to the hydroxylic peak, it may represent a

Figure 4: Photolysis of 1 at ambient temperature.

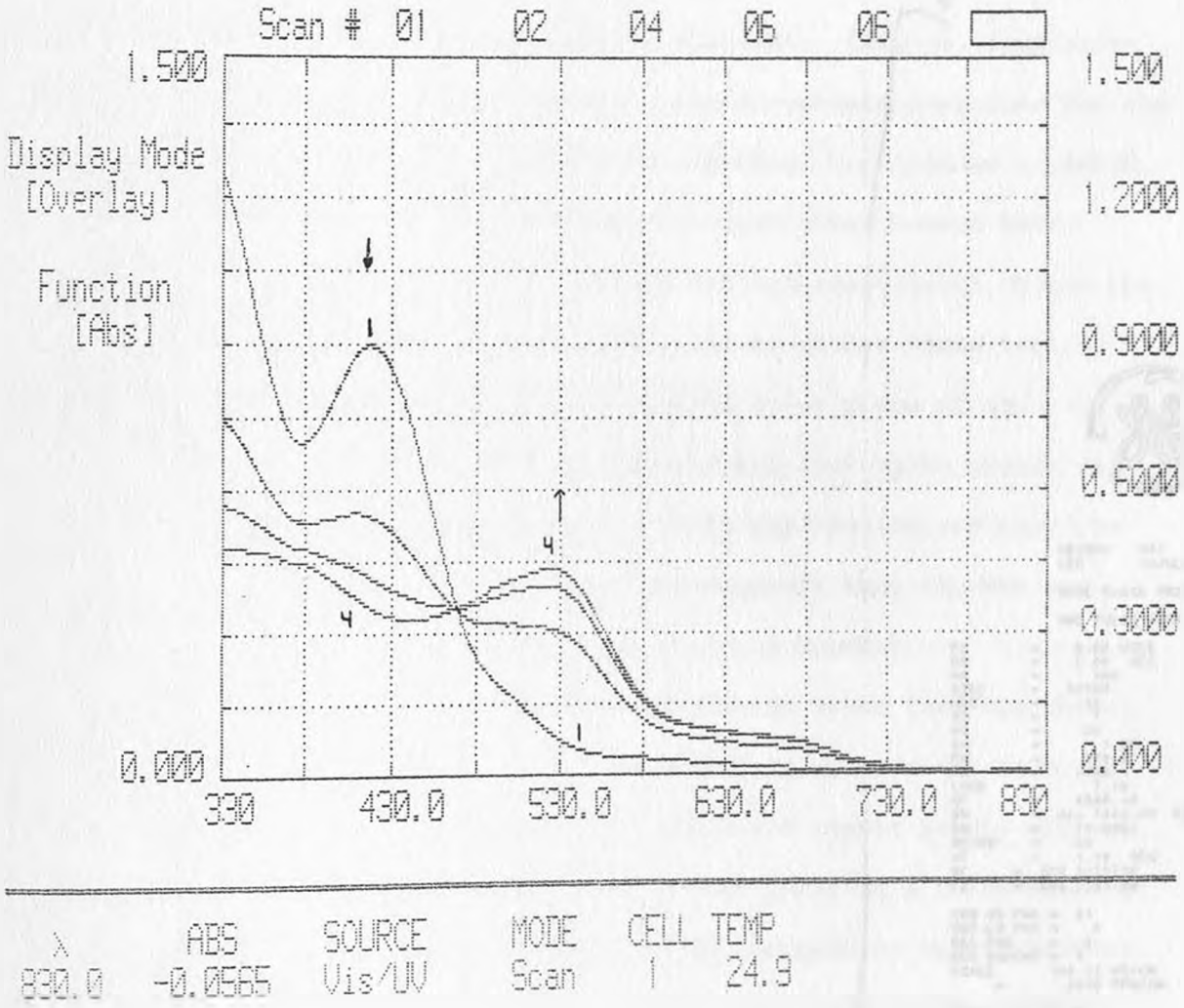

Figure 5: 500MHz ^{1}H NMR of 2.

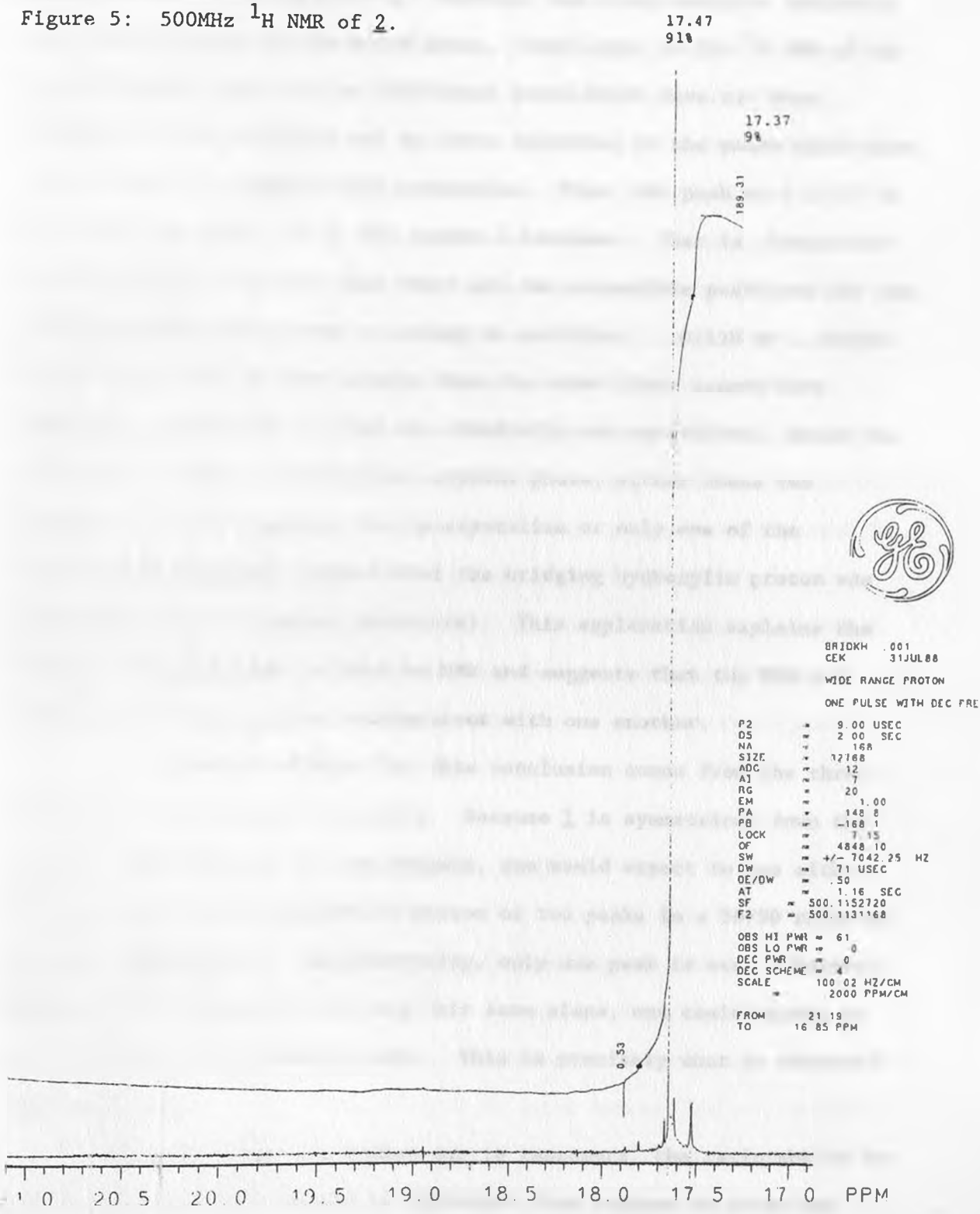

slightly different isomer of 2. However, the x-ray analysis indicates only one structure in the solid phase. Similarly, in the ^1H NMR of the solution phase there are no additional peaks which have not been assigned to the structure nor is there splitting in the peaks which have been assigned to support this conclusion. Thus, the peak at δ 17.37 is not likely an isomer of 2, but rather a tautomer. That is, inspection of 2 in Figure 3 reveals that there are two accessible positions for the bridging hydroxylic proton to occupy in solution, ...O(1)H or ...O(2)H. One of these must be more stable than the other (they cannot have identical stabilities as they are chemically non-equivalent), hence the 9/91 ratio. Then, in the solid, crystal phase, either these two slightly different species can co-crystalize or only one of the positions is possible (recall that the bridging hydroxylic proton was not located in the crystal structure). This explanation explains the presence of both peaks as seen by NMR and suggests that the NMR and crystal structure are not inconsistent with one another.

Further evidence for this conclusion comes from the three-dimensional structures of 1 and 2. Because 1 is symmetrical down the vertical axis between the two oxygens, one would expect to see either only one peak for the downfield proton or two peaks in a 50/50 ratio at very low temperature. Experimentally, only one peak is seen. However, since 2 is not symmetrical along this same plane, one could expect to see two peaks in an unequal ratio. This is precisely what is observed experimentally.

If the two peaks are indeed due to tautomers, the ratio should be solvent dependant (it should be different from benzene in polar and protic solvents). ^1H NMRs of 2 were taken in three different solvents;

methanol, acetone, and chloroform. In methanol no downfield protons were visible at all and the integrals of the upfield protons changed, suggesting that either decomposition had occurred or the iodide had dissociated, broadening the peaks of the NMR. In acetone one peak was present at δ 16.67 and in chloroform two peaks were present, one at δ 16.32 and one at δ 16.62. The peak at δ 16.62 was present in approximately 3% by integration. The solvent-dependant ratio of the two peaks further supports the presence of two hydroxylic proton tautomers.

The thermolysis of 2 in the presence of TEMPO free radical trap quantitatively yields trapped benzylTEMPO and the Co^{II}• ligand. The reaction proceeded cleanly by visible spectroscopy with an isosbestic point at 488 nm (Figure 6). The thermolysis product was compared to authentic benzylTEMPO synthesized independently. The yield by analytical gas chromatography was 95 ± 6% benzylTEMPO (see Appendix 3 for G.C. results and calculations). As was determined previously,[1] the thermolysis of 1 in the presence of TEMPO also quantitatively yields benzylTEMPO.

Equilibrium Studies

To authenticate the NMR integrals used in all subsequent kinetic studies performed on 1 and 2, it was necessary to verify that the aquisition times used in the NMR experiments are long enough so that the downfield protons have adequate time to relax between pulses, thereby giving accurate integral values. For a 1 second relaxation period, the mean fraction of 1 (ie. 1/1+2) was 0.22 ± 0.03. The mean fraction of 1 for a 10 second relaxation time was 0.20 ± 0.02. Within experimental

Figure 6: 69°C thermolysis of 2 with TEMPO trap.

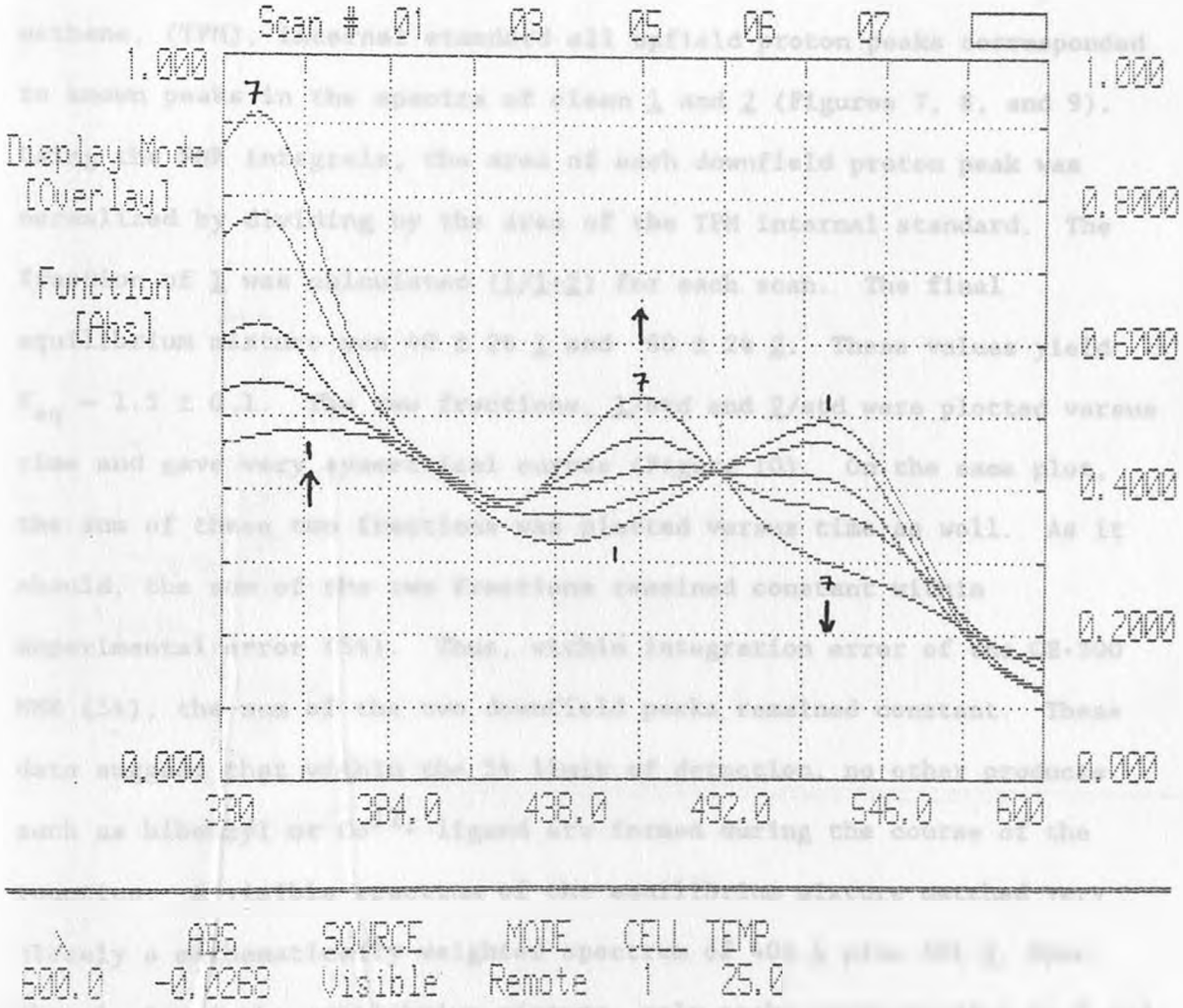

The thermolysis reaction was done over a period of approximately 30 hours. Admission of a trace amount of oxygen, resulting in slight decomposition, is likely the reason for the absence of an isosbestic point at 573 nm. The isosbestic point at 488 nm is likely less sensitive than the one at 573 nm, thus it remains clean even with trace amounts of oxygen present.

error, the fraction of 1 at two ten-fold different relaxation times is constant. Thus the default delay time of 1 second is sufficient to give reliable NMR integrals.

The 69°C thermolysis of 1 at NMR concentration was complete within ca. 30 hours by NMR. With the exception of the peak for triphenyl methane, (TPM), internal standard all upfield proton peaks corresponded to known peaks in the spectra of clean 1 and 2 (Figures 7, 8, and 9). Using the NMR integrals, the area of each downfield proton peak was normalized by dividing by the area of the TPM internal standard. The fraction of 1 was calculated (1/1+2) for each scan. The final equilibrium mixture was 40 ± 2% 1 and 60 ± 2% 2. These values yield K_{eq} = 1.5 ± 0.1. The two fractions, 1/std and 2/std were plotted versus time and gave very symmetrical curves (Figure 10). On the same plot, the sum of these two fractions was plotted versus time as well. As it should, the sum of the two fractions remained constant within experimental error (5%). Thus, within integration error of the QE-300 NMR (5%), the sum of the two downfield peaks remained constant. These data suggest that within the 5% limit of detection, no other products such as bibenzyl or Co^{II}• ligand are formed during the course of the reaction. A visible spectrum of the equilibrium mixture matched very closely a mathematically weighted spectrum of 40% 1 plus 60% 2. Upon photolysis of the equilibrium mixture, only peaks corresponding to 2 and TPM internal standard were visible by NMR, indicating that 2 was formed quantitatively. The visible spectrum of this photolysis product showed the characteristic spectrum of 2 with the λ_{max} at 525 nm (Figure 11).

The 69°C thermolysis of 2 at NMR concentration was complete within ca. 35 hours. The final NMR spectrum again showed peaks corresponding

Figure 7: ^{1}H NMR of 1 (bottom) and 2 (top).

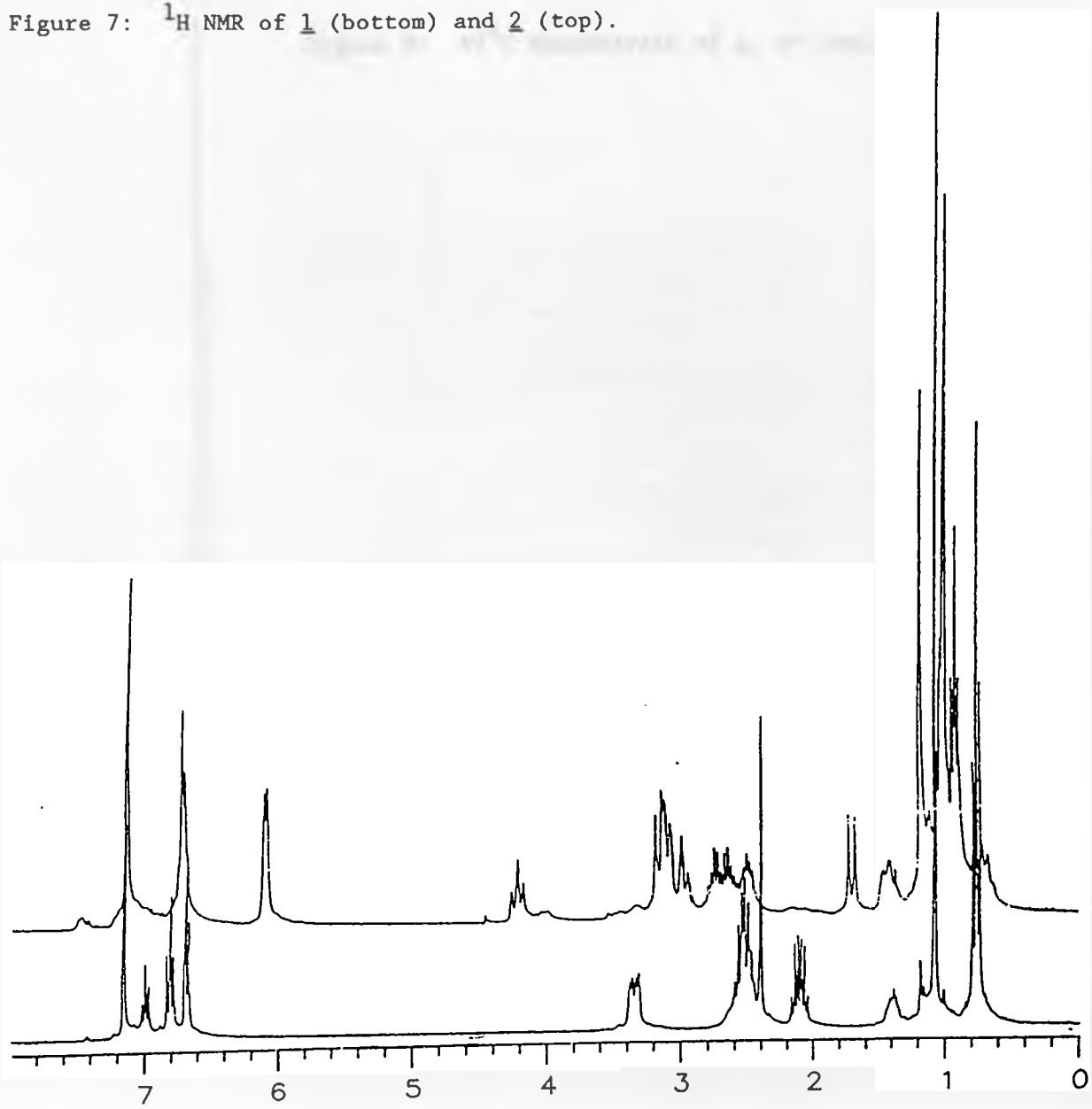

Figure 8: 69°C thermolysis of 1, at equilibrium.

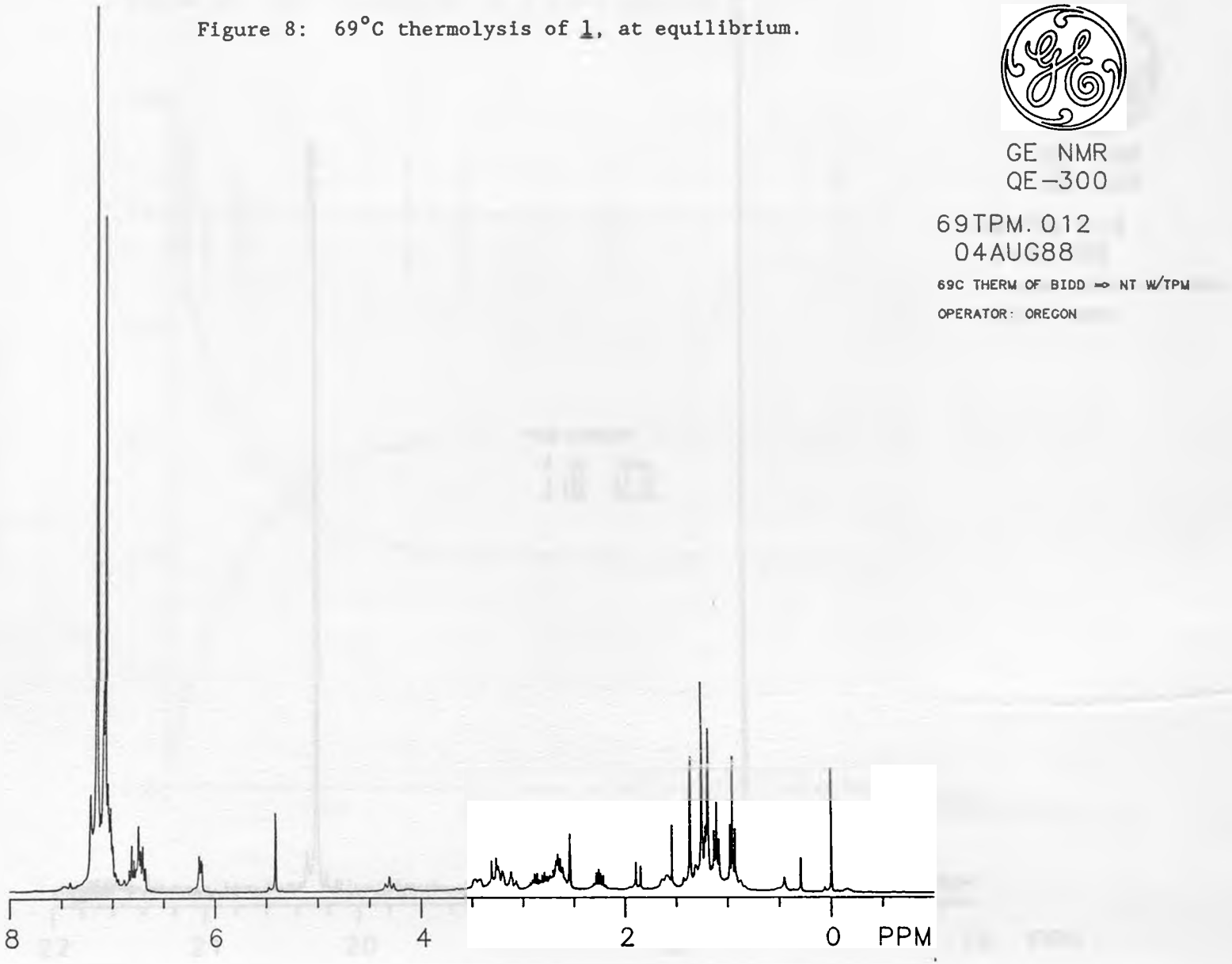

Figure 9: 69°C thermolysis of 1, at equilibrium.

GE NMR
QE-300

69TPM.012
04AUG88

69C THERM OF BIDD => NT W/TPM

OPERATOR: OREGON

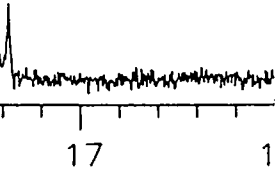

Figure 10: 69°C thermolysis of 1 and 2 with TPM.

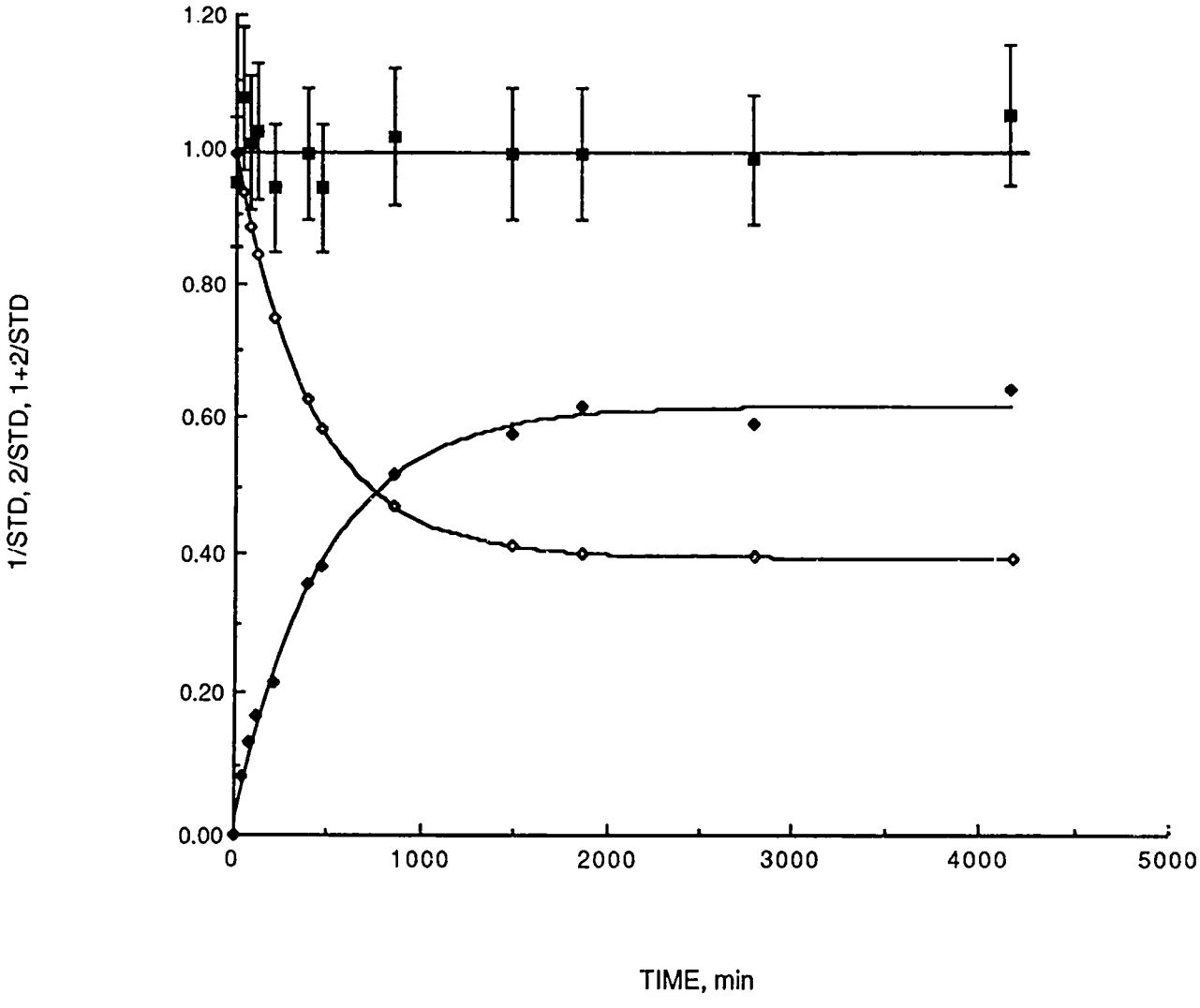

Figure 11: Visible spectra of 1 and 2.

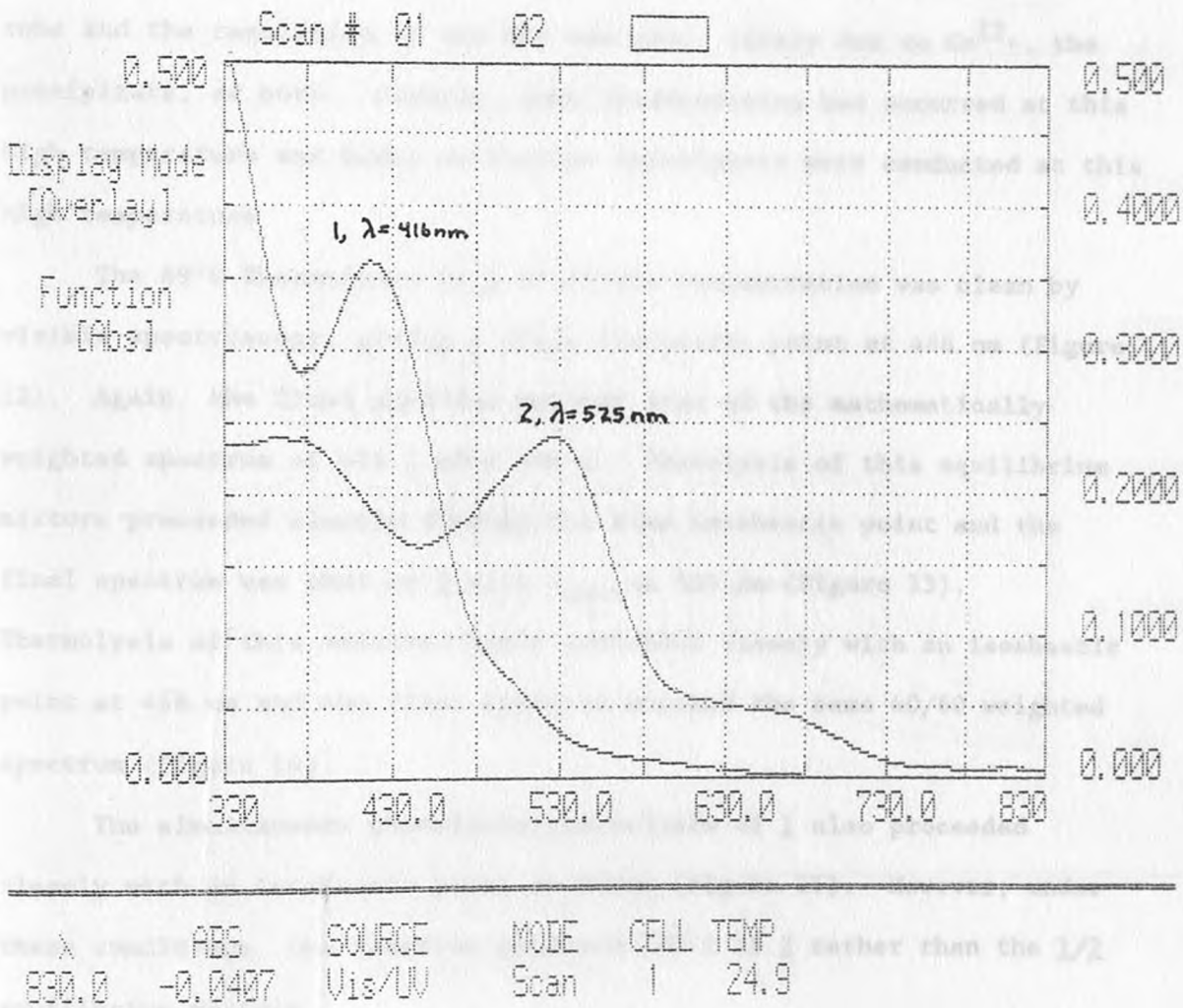

only to 1, 2, and TPM. Integration again gave the same 40 ± 2/60 ± 2 ratio. The visible spectrum of this equilibrium mixture also matched that of the mathematically weighted spectrum as above.

NMR concentration thermolysis of 1 at 85°C gave the same equilibrium mixture within 2%. However, precipitate was present in the tube and the resolution of the NMR was poor, likely due to Co^{II}•, the precipitate, or both. Clearly, some decomposition had occurred at this high temperature and hence no further experiments were conducted at this high temperature.

The 69°C Thermolysis of 1 at UV/vis concentration was clean by visible spectroscopy, giving a clean isosbestic point at 466 nm (Figure 12). Again, the final spectrum matched that of the mathematically weighted spectrum of 40% 1 plus 60% 2. Photolysis of this equilibrium mixture proceeded cleanly through the same isosbestic point and the final spectrum was that of 2 with λ_{max} at 525 nm (Figure 13). Thermolysis of this solution again proceeded cleanly with an isosbestic point at 466 nm and the final spectrum matched the same 40/60 weighted spectrum (Figure 14).

The simultaneous photolysis/thermolysis of 1 also proceeded cleanly with an isosbestic point at 466nm (Figure 15). However, under these conditions, the reaction produced 100 ± 5% 2 rather than the 1/2 equilibrium mixture.

Calculation of the 69°C thermolysis equilibrium constant (Appendix 1) gives $K_{eq69°} = 1.5 \pm 0.1$. This implies $\Delta G_{69°C} = -0.28 \pm 0.02$ kcal/mol. Assuming a near temperature-independent equilibrium, $\Delta H^o = 0$, $\Delta S^o = 0.82 \pm 0.06$ cal/mol•K and $\Delta H^o = 0.00 \pm 0.02$ kcal/mol. It thus appears that the thermolysis reaction is largely entropically driven.

Figure 12: 69°C thermolysis of 1 to equilibrium.

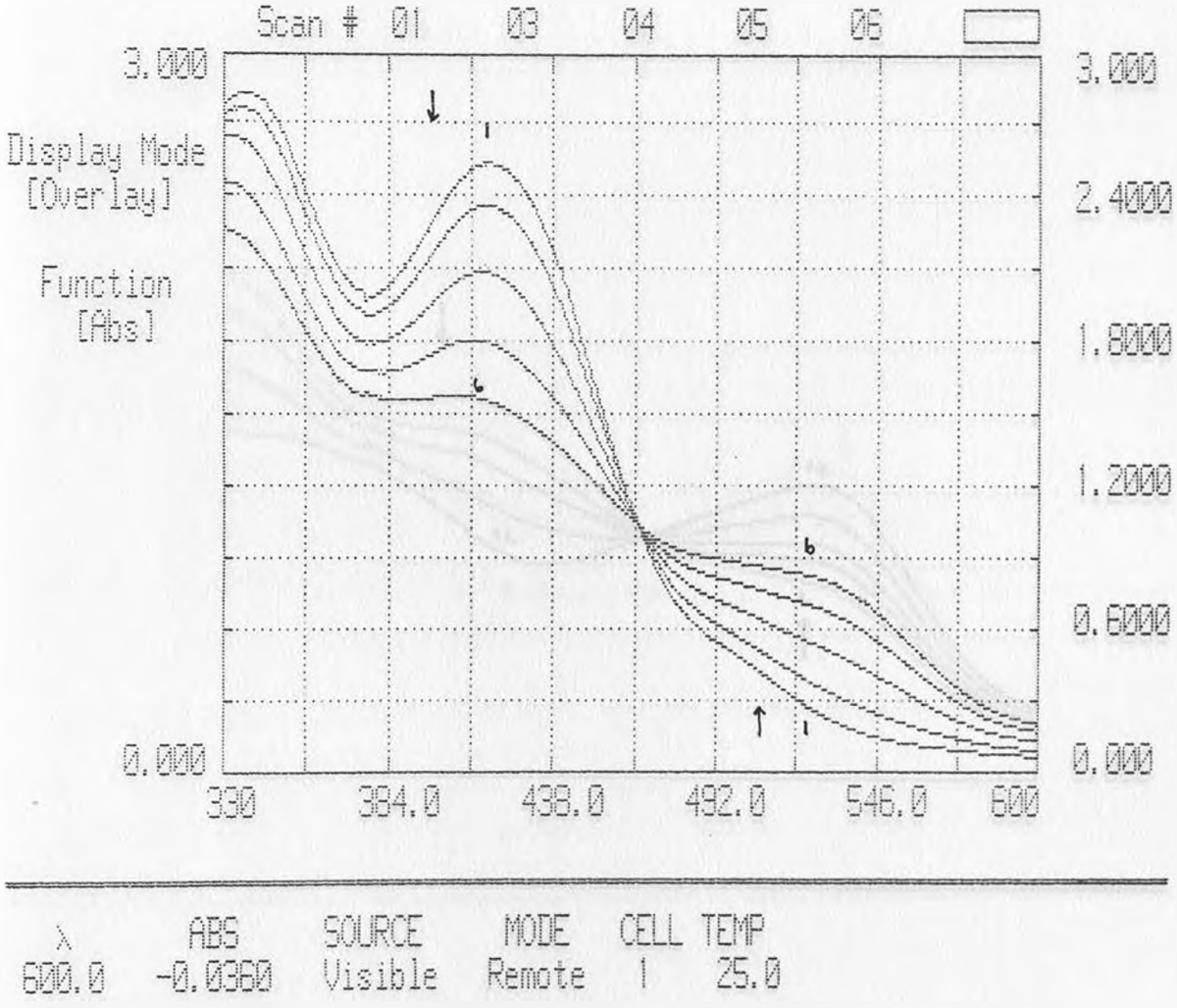

Figure 13: Photolysis of equilibrium mixture to 2.

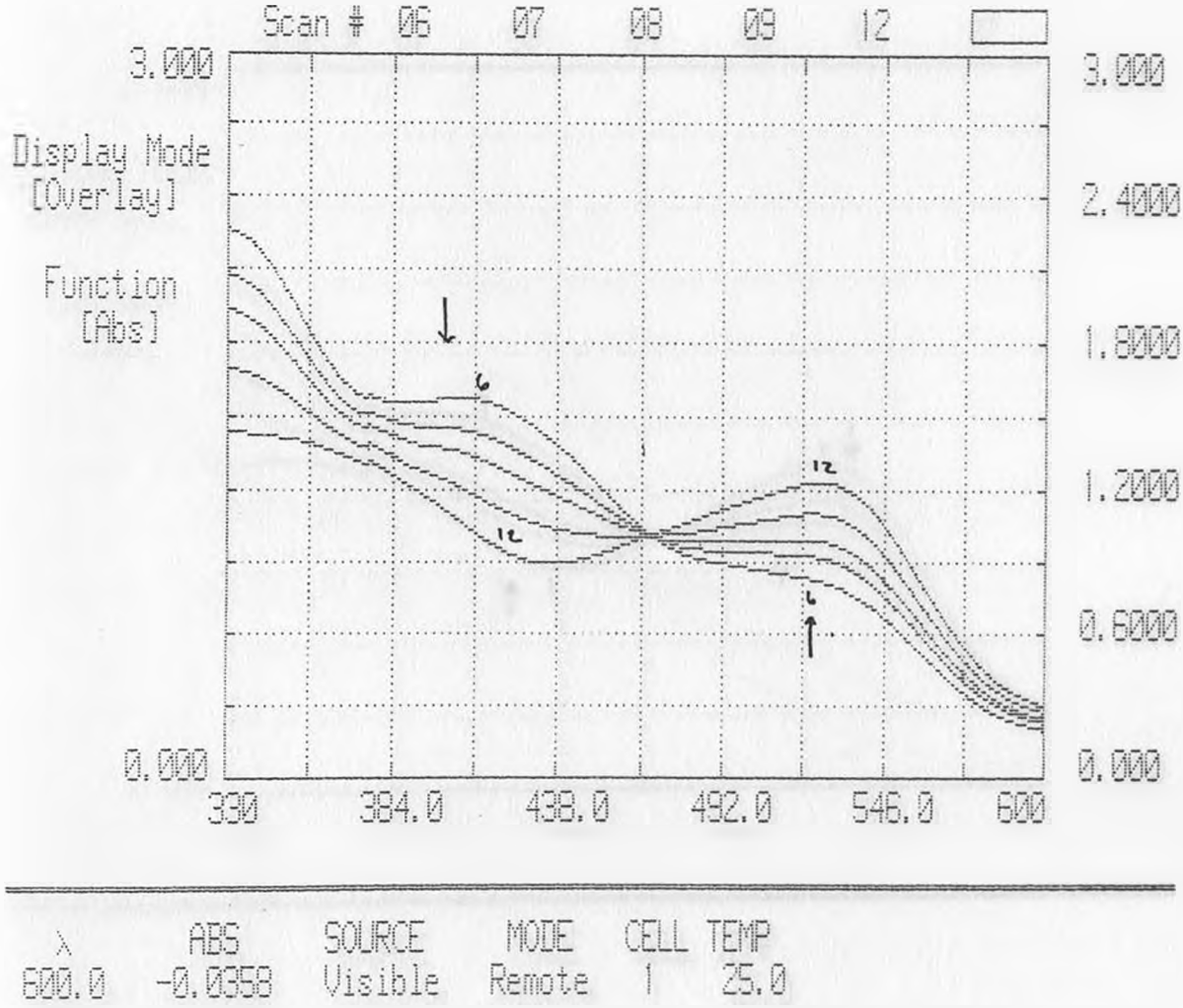

Figure 14: 69°C thermolysis of 2 to equilibrium.

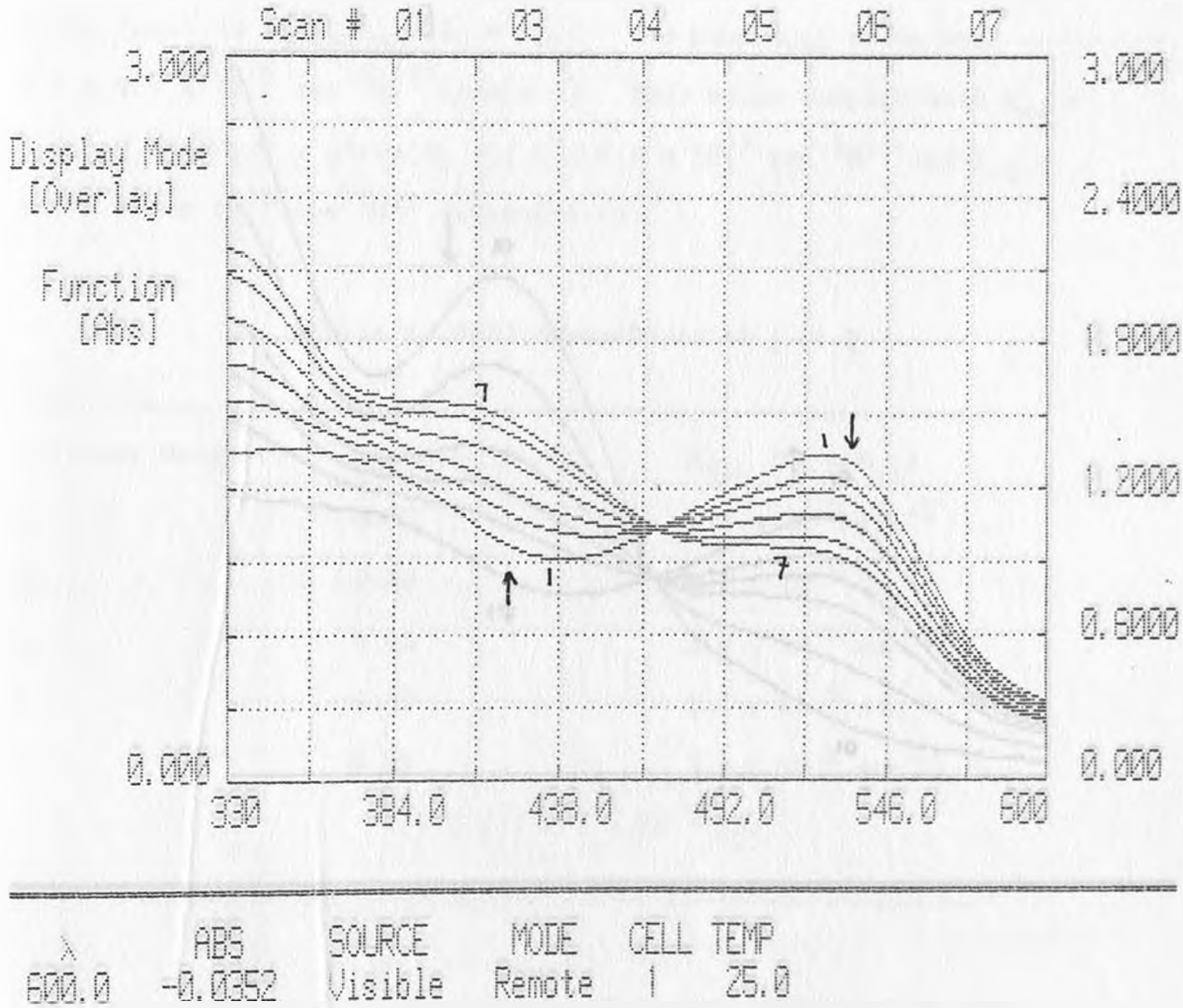

Figure 15: 69°C photolysis of 1.

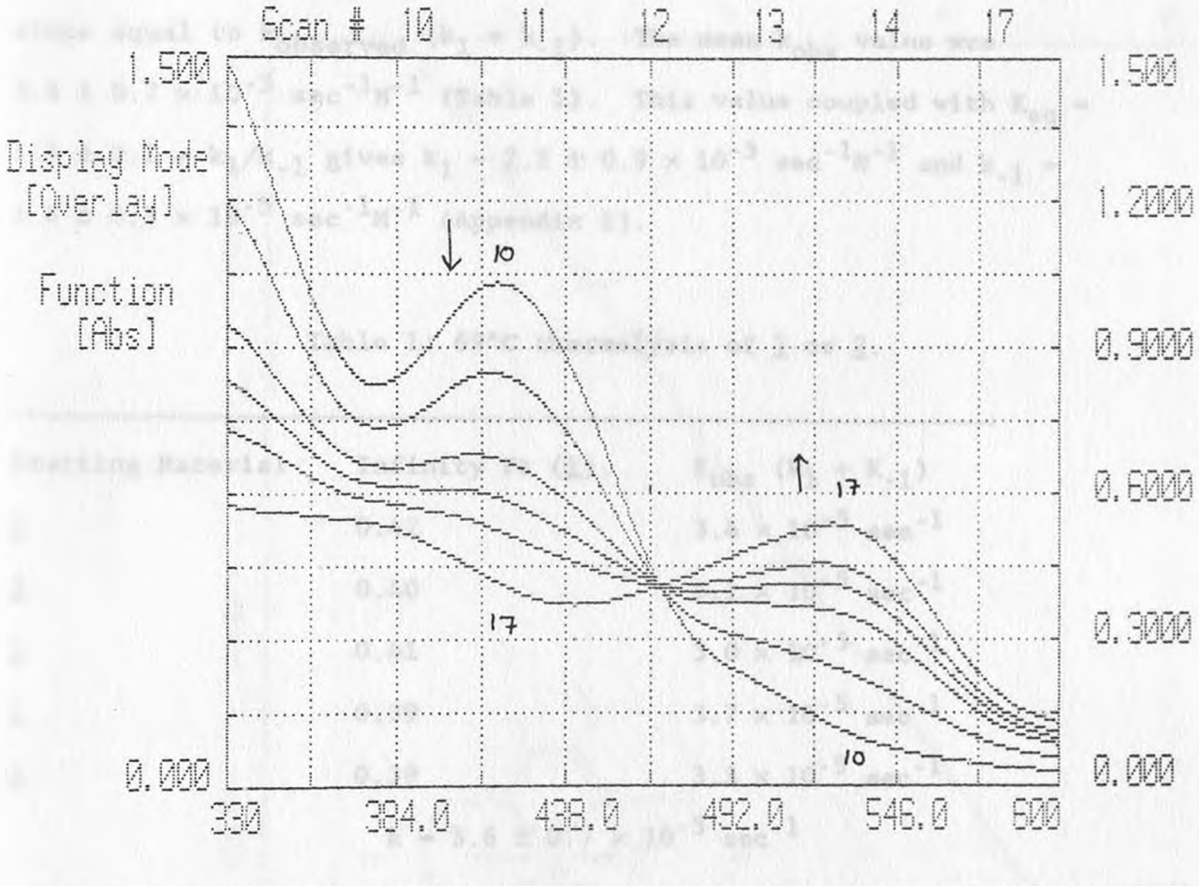

Kinetic Results

Plots of $\ln(A_t - A_\infty)$ versus time for the thermolysis of 1 and 2 are linear (Figures 16 and 17), indicating a first-order reaction, with the slope equal to $k_{observed}$ $(k_1 + k_{-1})$. The mean k_{obs} value was $3.6 \pm 0.7 \times 10^{-5}$ $sec^{-1}M^{-1}$ (Table 1). This value coupled with $K_{eq} = 1.5 \pm 0.1 = k_1/k_{-1}$ gives $k_1 = 2.2 \pm 0.9 \times 10^{-5}$ $sec^{-1}M^{-1}$ and $k_{-1} = 1.4 \pm 0.3 \times 10^{-5}$ $sec^{-1}M^{-1}$ (Appendix 1).

Table 1: 69°C thermolysis of 1 or 2.

Starting Material	Infinity Pt (1).	K_{obs} $(k_1 + K_{-1})$
1	0.42	3.4×10^{-5} sec^{-1}
2	0.40	5.1×10^{-5} sec^{-1}
1	0.41	3.0×10^{-5} sec^{-1}
1	0.39	3.7×10^{-5} sec^{-1}
2	0.39	3.3×10^{-5} sec^{-1}
	$k = 3.6 \pm 0.7 \times 10^{-5}$ sec^{-1}	

The rates for the thermolysis of 2 with TEMPO trap at four different temperatures at zero order TEMPO are given in table 2 (a plot of $\ln(A_t - A_\infty)$ vs. T was linear indicating the reaction is first order overall, and thus zero order in TEMPO, Figure 18). The pseudo first-order rate constant for this reaction extrapolated to 69°C is 1.6×10^{-5} sec^{-1}, 31 times smaller than the pseudo first-order rate constant for

Figure 16: 69°C thermolysis of 1 to equilibrium.

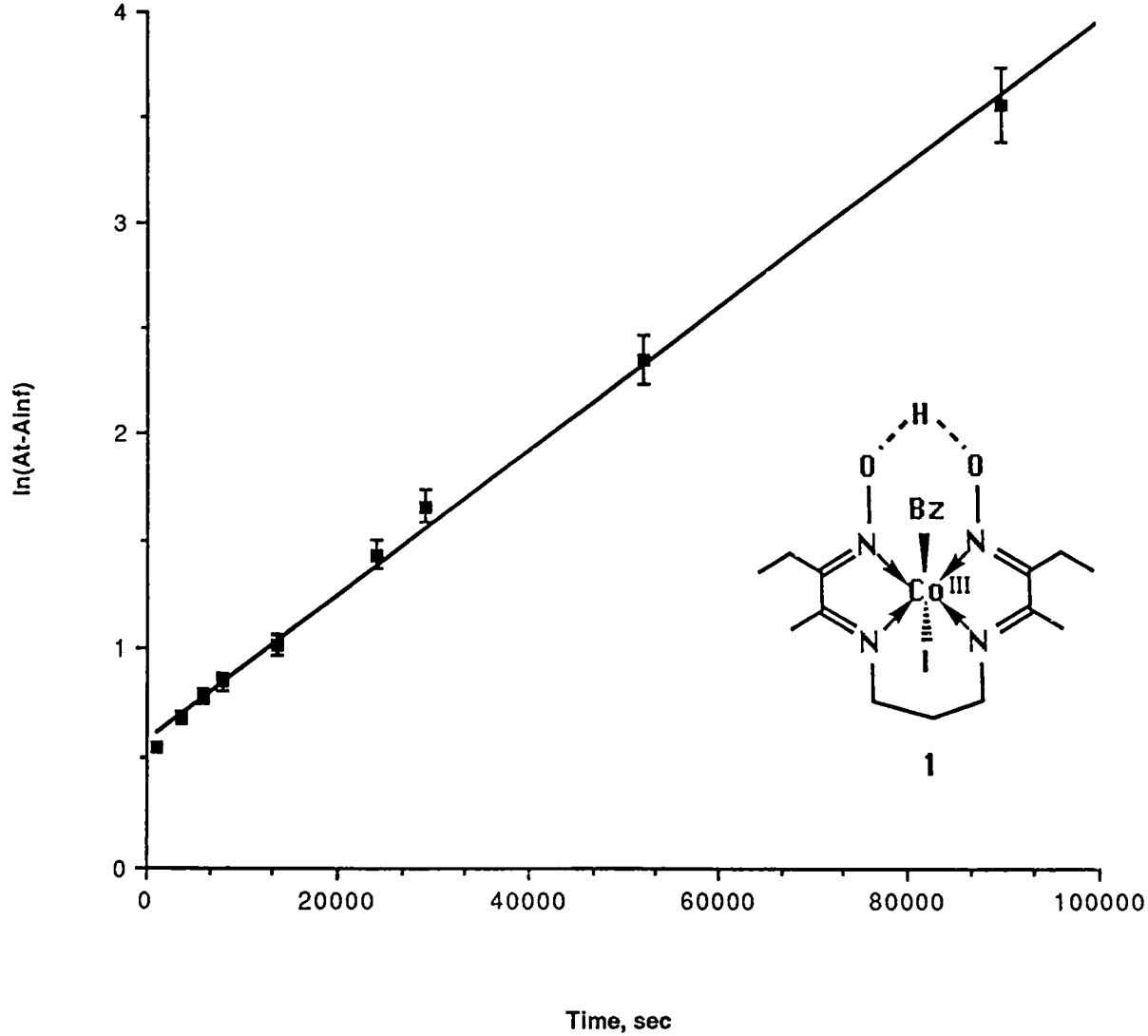

Figure 17: 69°C thermolysis of 2 to equilibrium.

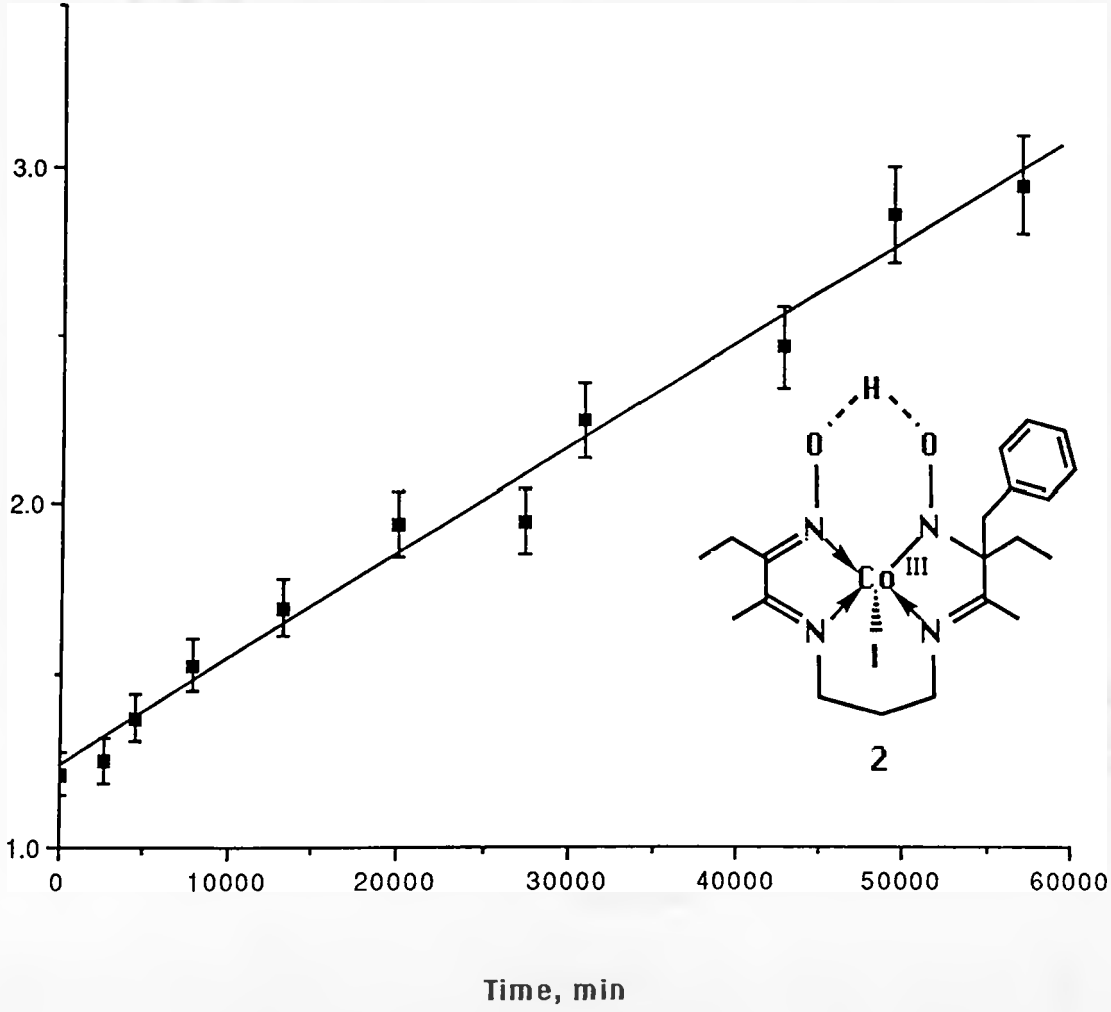

Figure 18: 69°C thermolysis of 2 with TEMPO trap.

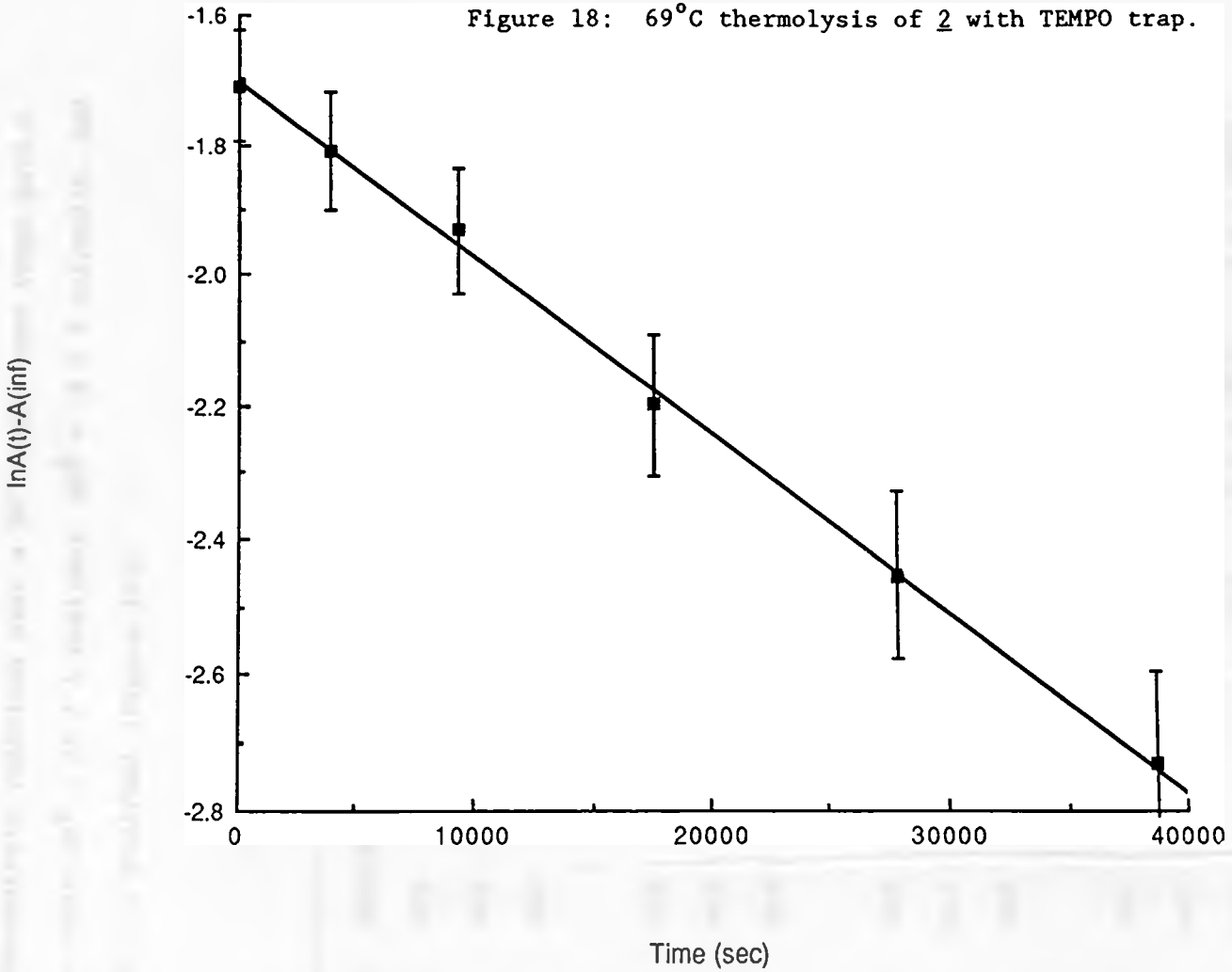

the thermolysis of 1 with TEMPO.[1] An Arrhenius plot of ln k vs. 1/T for the four thermolysis reactions over a 30° temperature range gave a linear plot with $\Delta H^{\ddagger}$ = 25 ± 1 kcal/mol, $\Delta S^{\ddagger}$ = -8 ± 3 cal/mol·K, and $\Delta G^{\ddagger}_{298}$ = 27 ± 1 kcal/mol (Figure 19).

Table 2: Thermolysis of 2 with TEMPO.

Experiment	Abs(nm)	min(95%)	k sec^{-1}	max(95%)
2 + TEMPO	526	3.9×10^{-6}	6.2×10^{-6}	1.0×10^{-5}
at	462	3.6×10^{-6}	4.6×10^{-6}	6.0×10^{-6}
60°C	340	5.1×10^{-6}	6.0×10^{-6}	6.8×10^{-6}
		$k = 5.6(8) \times 10^{-6}$ sec^{-1} (1δ)		
2 + TEMPO	526	1.6×10^{-5}	2.0×10^{-5}	2.5×10^{-5}
at	462	1.6×10^{-5}	2.0×10^{-5}	2.3×10^{-5}
70°C	340	2.0×10^{-5}	2.1×10^{-5}	2.3×10^{-5}
		$k = 2.0(0) \times 10^{-5}$ sec^{-1} (1δ)		
2 + TEMPO	526	2.5×10^{-5}	3.5×10^{-5}	5.0×10^{-5}
at	462	1.6×10^{-5}	2.6×10^{-5}	4.3×10^{-5}
75°C	340	1.7×10^{-5}	2.6×10^{-5}	4.0×10^{-5}
		$k = 2.9(6) \times 10^{-5}$ sec^{-1} (1δ)		
2 + TEMPO	526	7.1×10^{-5}	1.3×10^{-4}	2.5×10^{-4}
at	462	-------	1.4×10^{-4}	-------
90°C	340	7.1×10^{-5}	1.4×10^{-4}	3.0×10^{-4}
		$k = 1.4(5) \times 10^{-5}$ sec^{-1} (1δ)		

Figure 19: Thermolysis of 2 with TEMPO trap (60-90°C).

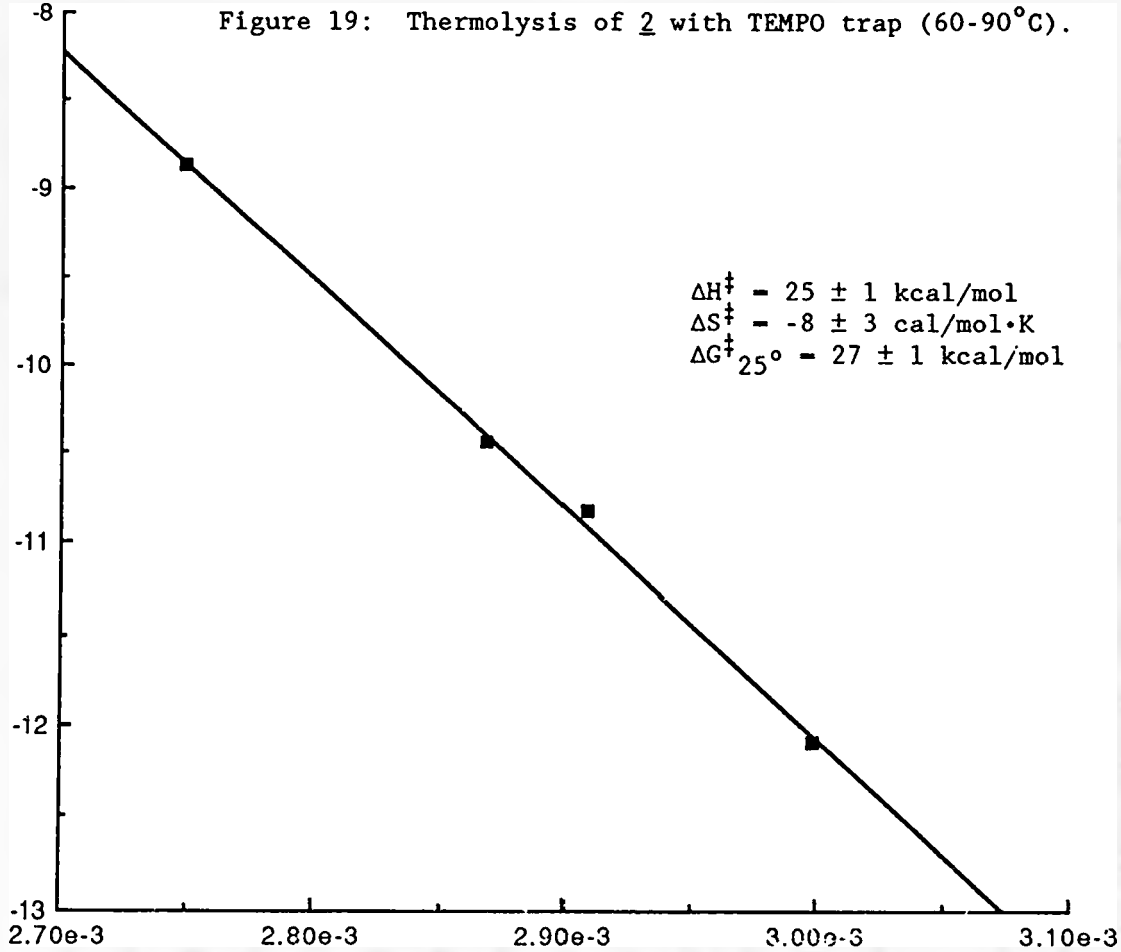

DISCUSSION

The goal of the research presented herein has been twofold: to completely characterize and unequivocally determine the structure of the novel rearrangement product 2; to perform kinetic and equilibrium studies, leading to a proposed mechanism for the formation of 2, consistent with all the experimental results. A summary of the results achieved are given below (Scheme 2):

Preliminary NMR evidence suggested that the benzyl group has migrated to somewhere on the equatorial ligand. The chemical literature supported this conclusion, but suggested a migration to nitrogen. However, the single most important piece of structural evidence, the x-ray diffraction crystal structure, demonstrates a migration to carbon, a completely novel result.

Compound 2 is formed quantitatively from 1 by anaerobic photolysis at ambient temperature. The reaction is clean by both NMR and visible spectroscopy. The product can be isolated as dark red microcrystals.

Thermolysis of 1 or 2 cleanly yields a near temperature-independent equilibrium mixture of 1 and 2 in a 40:60 ratio, respectively. It thus appears that the formation of 2 is largely entropically driven and is thus the thermodynamically favored product, while 1 is the kinetically favored product during its initial oxidative-addition synthesis from the Co(I) ligand and benzyl iodide.

Scheme 2

Summary of Results

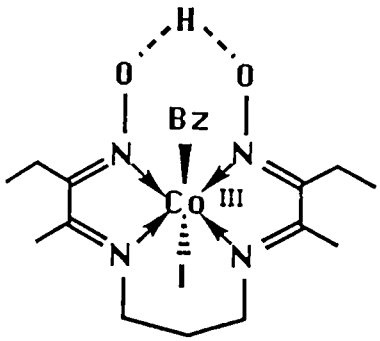

1

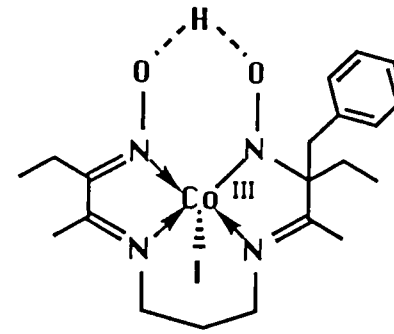

2

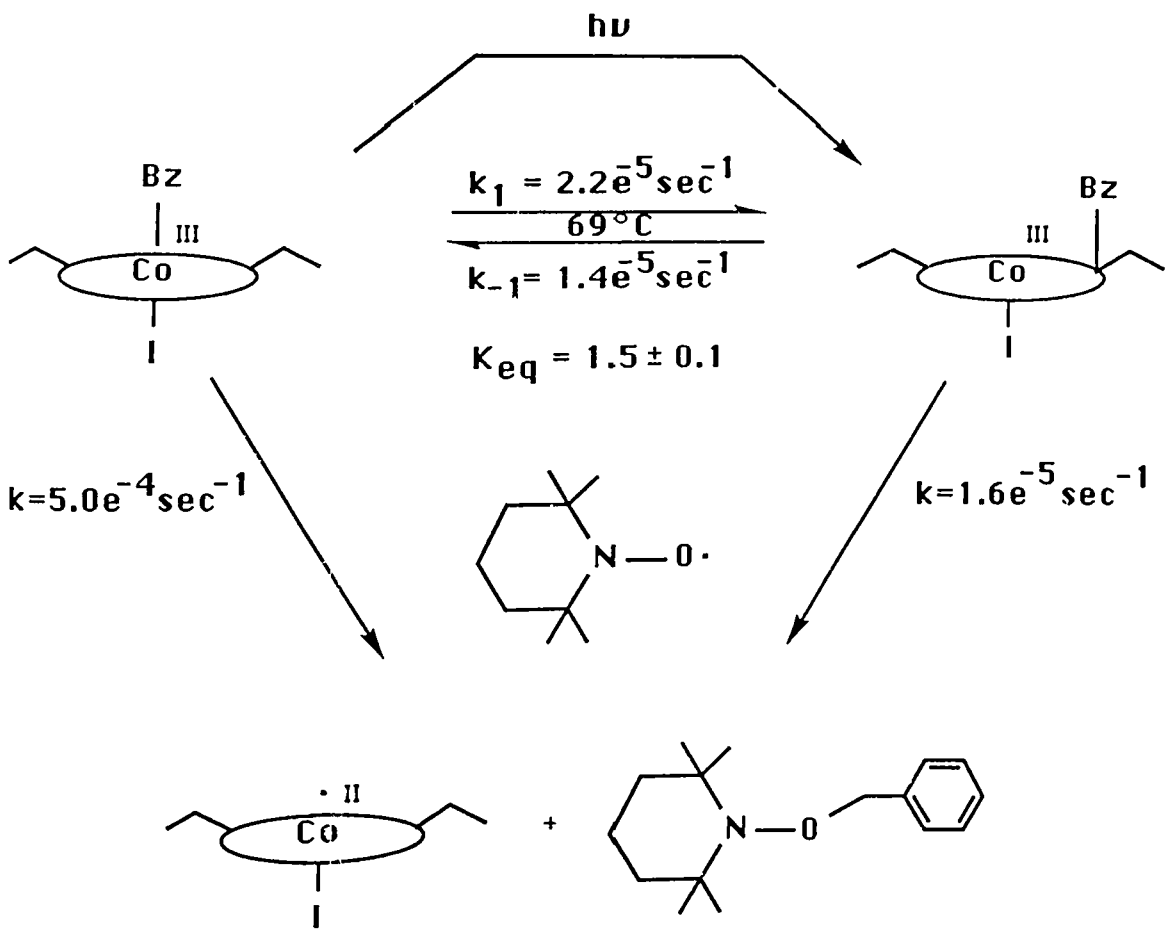

The thermolysis of 1 or 2 in the presence of TEMPO free radical trap quantitatively yields the Co^{II}• ligand and trapped benzylTEMPO, indicating the presence of free radicals, which in turn implies a radical solvent-cage escape step in the mechanism. In the absence of trap, no bibenzyl is observed, however (within the detection limits of the NMR and G.C.). These two results are seemingly contradictory as bibenzyl is a well known, highly stable recombination product of benzyl radicals. There is, however, precendence for the inability to observe bibenzyl in work by Fischer[11]. Fischer found that radical reactions involving two or more intermediates may lead to the specific formation of only one product if one species is more persistent than the others, and if persistent (Co(II)•) and transient ($C_6H_5CH_2$•) species are generated with equal rates. This is caused by an initial buildup of the persistent intermediate, which thereafter steers the system to follow a single path. The system studied, interestingly enough, was a B_{12} system; the photolysis of methylcobalamine in the presence of MCO. This reaction yielded acetylcobalamine in high yield and the following mechanism was suggested:

CH_3-cbl → •CH_3 + •cbl 1

•CH_3 + •cbl → CH_3-cbl 2

•CH_3 + CO → CH_3CO• 3

CH_3CO• + •cbl → CH_3CO-cbl 4

If these mechanisms were in fact occurring, it was surprising that the selectivity for them would be so high since reactions involving •CH_3 and CH_3CO• are known to self-terminate with high rate constants, hence one would intuitively expect the formation of the self-termination products to compete effectively with the cross-termination step to produce the

desired product. The following explanation was given to explain the results. In the photolysis reaction, a persistent radical, •cbl, is formed, along with the transient species $\cdot CH_3$ and $CH_3CO\cdot$. If some self-termination of the transient species occurs (CH_3-CH_3, $CH_3C(O)$-$CH_3C(O)$), the concentration of the persistent species will increase in time to high levels and subsequently steer the system towards cross-termination. In effect, the self-termination of the transient species (a fast process), will be suppressed by the slow self-determination of the persistent species (cbl-cbl). Thus, in order to form the cross-termination product, the rate of the cross-termination reaction must be greater than the geometric mean of the rates of the self-termination reactions. This model can be used to explain our inability (<5%) to find the self-termination product bibenzyl ($C_6H_5CH_2$-$CH_2C_6H_5$). When 1 or 2 is photolysed or thermolysed, benzyl radical and the $Co^{II}\cdot$ ligand are formed. A small amount of bibenzyl is likely formed (too small to detect), and $Co^{II}\cdot$ builds up. The competing reactions are then:

$$2Co^{II}\cdot \rightarrow Co^{II}\text{-}Co^{II} \quad (k_5 \approx 0, \text{ the product is unstable}) \qquad 5$$

$$2C_6H_5CH_2\cdot \rightarrow C_6H_5CH_2\text{-}CH_2C_6H_5 \quad (k_6 \text{ very fast}) \qquad 6$$

$$C_6H_5CH_2\cdot + Co^{II}\cdot \rightarrow \underline{1} \text{ or } \underline{2} \quad (k_7 \text{ slow}) \qquad 7$$

Because experimentally it is found that 1 or 2 are formed quantitatively, k_7 is thus necessarily greater than the geometric mean of k_5 and k_6.

Finally, all thermolysis reactions with either 1 or 2 demonstrate first-order kinetics. This key piece of evidence eliminates mechanisms similar to those by Kochi and Espenson discussed in the introduction as possibilities for the mechanism working in this case.

Thus, the simplest mechanism consistent with all of the experimental data is depicted in Scheme 3. In this mechanism, the cobalt-carbon bond (in the case of 1) or the carbon-carbon bond (in the case of 2) homolyzes, yielding a caged radical pair (k_1 or k_2). At this point, the two species are indistinguishable. It is possible that when the caged radicals are in close proximity of one another, the benzyl radical occupies an intermediate η^3 position (there is literature precedence for this possibility,[12] but because in this instance there is no evidence for it, it cannot be assumed). Next, the caged radical pair can recombine to form either 1 or 2 (k_{-1} or k_{-2}), or reversibly escape the cage to become free radicals (k_3 and k_{-3}). If TEMPO trap is present, the benzyl radical can then be irreversibly trapped (k_4), giving benzylTEMPO and the Co^{II}• ligand.

Some very remarkable results have been achieved from this research. From radical trapping studies of 2 with TEMPO, the homolysis bond dissociation energy of the carbon-carbon had been determined to be ≈23 ± 1 kcal/mol. The general equation for the bond dissociatiion energy is BDE = $\Delta H^{\ddagger}_{obs}$ - $F_c\Delta H^{\ddagger}_{\eta}$.[13] Assuming an efficient cage (F_c = 1) and $\Delta H^{\ddagger}_{\eta}$ ≃ 2 kcal/mol for benzene[13], this equation reduces to BDE = $\Delta H^{\ddagger}_{obs}$ - 2 kcal/mol. This result is quite interesting for two reasons. First, the average homolysis BDE for a 3° carbon-3° carbon is 77 kcal/mol (ie. tBu-tBu), and that for a benzyl-carbon bond is on the order of 76 kcal/mol.[14] Clearly, the BDE of the benzyl-carbon bond in 2 is much less, indicating that the bond is highly activated. Second, the cobalt-carbon homolysis BDE of 1 was previously[1] determined to be ≈26 ± 1 kcal/mol. *Thus, not only is the carbon-carbon bond in 2 weaker than the average benzyl-carbon bond by a considerable amount, it is*

Scheme 3

A possible mechanism

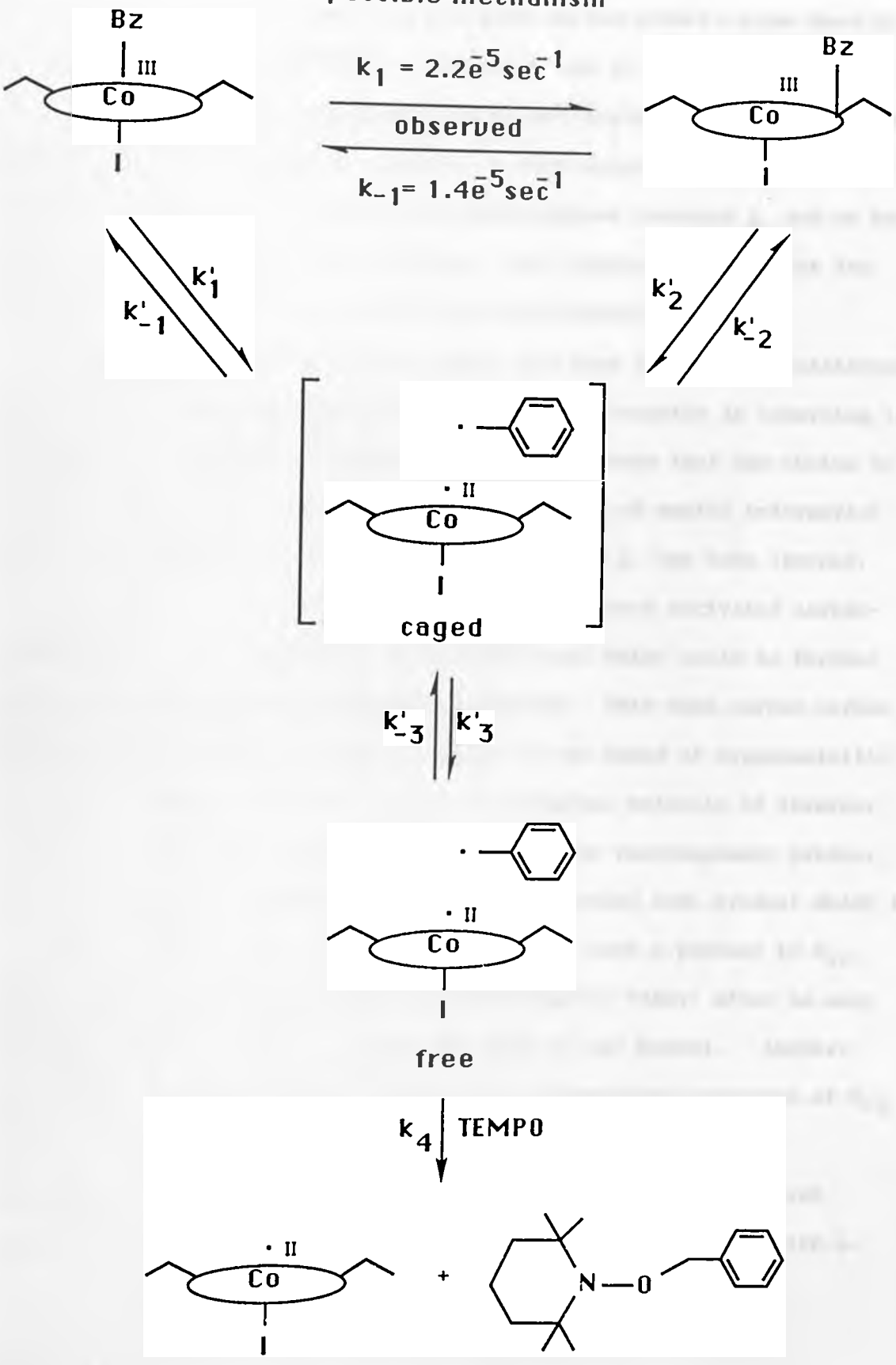

essentially the same strength (weakness!) as the cobalt-carbon bond in 1. This result was completely unexpected, and is very interesting.

The results presented herein have satisfactorily accomplished the goals they were intended to; namely, we have experimentally completely and successfully characterized the rearrangement compound 2, and we have proposed the simplest, and we believe, most-likely mechanism for its formation that is consistent with all experimental data.

The system studied is very clean, and thus it has been relatively easy to get at the chemistry and determine what exactly is occurring in this system - experienced mechanistic chemists know that the choice of their system is key. As a result, a great deal of useful information about the chemistry of the two compounds, 1 and 2, has been learned. For example, we have now learned how to make a very activated carbon-carbon bond. This could be a very useful tool which could be further exploited by techniques in organic synthesis. This weak carbon-carbon bond could also prove to be very useful in the field of organometallic chemistry. And in relation to B_{12}, the original molecule of interest, from which this work came, the structure of the rearrangement product, 2, could very well resemble a catalyst degradation side product which is no longer active. There is no precedence for such a product in B_{12} chemistry, but it could explain why the cofactor "dies" after so many turnovers (if - in fact - it does so; this is not known). Another possibility is that 2 could represent an intermediate structure of B_{12} which is the catalytically active species, but not physically observable. In particular, one could replace the cobalt-centered cobalt-participation question in mechanistic B_{12} chemistry[15] with a

carbon-centered B_{12}-centered participation question. This possibility has never before been realized.

EXPERIMENTAL

General

Reagents

Unless otherwise noted, all laboratory reagents were used as received without further purification. Benzene was distilled under N_2 over CaH_2. Deuterobenzene (99.6%D), Cambridge Isotopes was degassed by bubbling with N_2 for 1/2 hour. $Co[(DO)(DOH)_{pn}]I_2$ was synthesized by Gray[16] and gave satisfactory elemental analysis and NMR and visible spectra. TEMPO free radical (Aldrich) was purified by water aspirator vacuum sublimation at ambient temperature (mp = 33°C, lit. = 33°C).[17] Benzyl Iodide (ICN Biomedicals Inc., K & K Labs) gave a satisfactory NMR spectrum and was bubbled with N_2 for 1/2 hour. Carbon Monoxide and house nitrogen were scrubbed for water (4Å molecular seives) and O_2 (BASF copper catalyst in the black, reduced form).

Equipment

Proton NMR spectra, referenced to the benzene protic impurity, δ 7.15, were recorded on GE QE-300 and GN 500 MHz spectrometers. Ultraviolet and visible spectra were measured using a Beckman DU-7 spectrometer. Preparative gas chromatography was done using a Varian Aerograph Series 2700 GC with a 1.5% 100/120 OV-101 column. Analytical

gas chromatography was done using a Hewlett Packard 5790A Series GC with an Alltech Econo-cap carbowax capillary column, 30m x 0.25mm I.D., df = 0.25μm. Mass spectra were recorded on a VG-12-250 mass spectrometer, 70 ev positive-ion mass spectrum.

Air-sensitive Technique

All air-sensitive compounds were manipulated either by Schlenk technique or in the glove box. The glove box is an inert atmosphere, double-length, nitrogen-containing box (Vacuum Atmospheres). Oxygen levels averaged 0.3 ppm. Air-free transfers outside the box were done by either gas-tight syringe or stainless steel cannula. Spectra of air-sensitive compounds were taken in either pyrex cuvettes fitted with airtight teflon screw caps (Kontes) or NMR tubes fitted with airtight teflon screw caps (J. Young).

Light-sensitive Technique

All light-sensitive compounds were protected from exposure to light by either aluminum foil or black electrician's tape. Transfer of these compounds was done in the dark or with absolute minimal exposure to room light.

Quenching technique

All cuvettes and NMR tubes containing samples used in thermolysis reactions (69-85°C) were first quenched by cooling in room-temperature water for at least five minutes before spectra were taken.

Preparation of Compounds

$Co^{I}[(DO)(DOH)_{pn}]CO$: (Trimethylenedinitrilo)-bis(3-oximato-2-pentanone)cobalt(I) was prepared by the method of Finke et al.[18] Under reducing conditions, CO was bubbled through a solution of $Co[(DO)(DOH)_{pn}]I_2$ in 10% MeOH/NaOH. After bubbling one hour, the solvent was pumped off under vacuum and the brown microcrystaline product was washed with water, dried, and collected. Yields for three separate preparations were 0.7473g (49%), 1.0530g (70%), and 0.9643g (63%). Purity was determined to be >95% by NMR in agreement with the literature. Elemental analysis: calculated 47.4% C, 6.5% H, 15.8% N; found 46.58% C (carbon consistently gives a poor analysis for this compound), 6.35% H, 15.75% N.

$C_6H_5CH_2Co^{III}[(DO)(DOH)_{pn}]I$, 1,: Transbenzyliodo(trimethylenedinitrilo)-bis(3-oximato-2-pentanone)cobalt$^{(III)}$ was prepared by the method of Gray.[16] Three to five equivalents of benzyl iodide were used. The benzyl iodide oxidatively adds to the $Co^{I}[(DO)(DOH)_{pn}]CO$; the reaction is complete instantaneously. Yields for four separate preparations were 0.6173 g (50%), 0.3963 g (72%), 0.5171 g (95%), and 0.9632 g (91%). Purity was

determined to be >95% by NMR and visible spectroscopy in agreement with the literature. Elemental analysis: calculated 44.1% C, 5.5% H, 10.3% N; found 44.15% C, 5.44% H, 10.18% N.

(SP-5-15)-[2[[3-[[2-(hydroxyamino)-1-methyl-2-(phenylmethyl)butylidene]-amino]propyl]imino]-3-pentanone oximato(2-)-N,N',N'',N''']iodocobalt, 2: In the drybox 197 mg of 1 were dissolved in 95 mls of benzene in a 300 ml round bottom flask fitted with a rodaviss joint without grease. The flask was sealed and brought out of the box. The flask was secured above a foil plate, 30 cm below a GE sunlamp. Cool air was blown over the flask continually (Figure 20). The flask was photolysed for ca. 48 hours. The flask was taken back into the box and 5 mls was removed and rotoevaporated to dryness. The dry product was dissolved in ca. 2 mls of deuterated benzene, transferred to, and sealed in an airtight NMR tube. Evaluation by NMR showed the reaction to be complete. The benzene was rotoevaporated off outside the box. The product was scraped out of the flask, placed in an amber vial, aerated with N_2 for 1/2 hour, and placed in the freezer. Yields for six separate preparations: 0.1246 g (54%), 0.1093 g (53%), 0.0702 g (32%), 0.0466 g (23%), 0.1970 g (63%), and 0.1104 g (41%). All preparations showed 100% reaction by NMR (1 peak at δ 20.24 completely gone), but it was difficult to collect all of the product, thus the low yields. ^{1}H NMR (benzene-d_6) δ 1.1(m,6H), 1.2(m,3H), 1.3(m,3H), 1.6(m,2H), 1.9(d,1H), 2.6(m,2H), 2.8(m,2H), 2.9(m,2H), 3.1(m,1H), 3.3(m,1H), 4.3(t,1H), 6.1(d,2H), 6.7(m,3H), 17.5(s,1H). ^{13}C NMR (benzene-d_6) δ 10.32(C_9), 11.00(C_{13}), 15.32(C_{10}), 16.66(C_{11}), 21.20(C_{14}), 26.93(C_3 or C_4 or C_5), 30.14(C_3 or C_4 or C_5), 38.08(C_3 or C_4

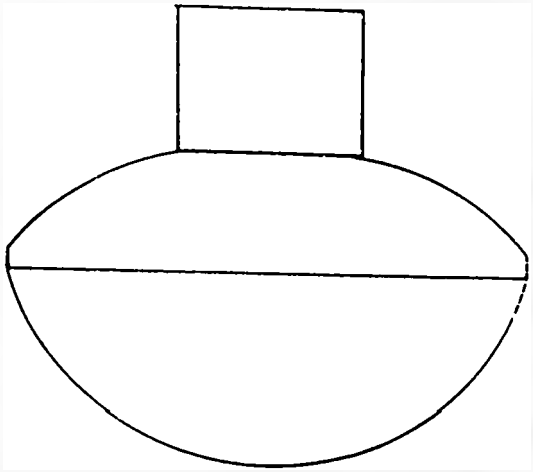

Figure 20: Experimental setup for the preparation of 2.

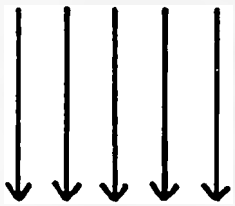

Ultraviolet light (hν)

Cool air

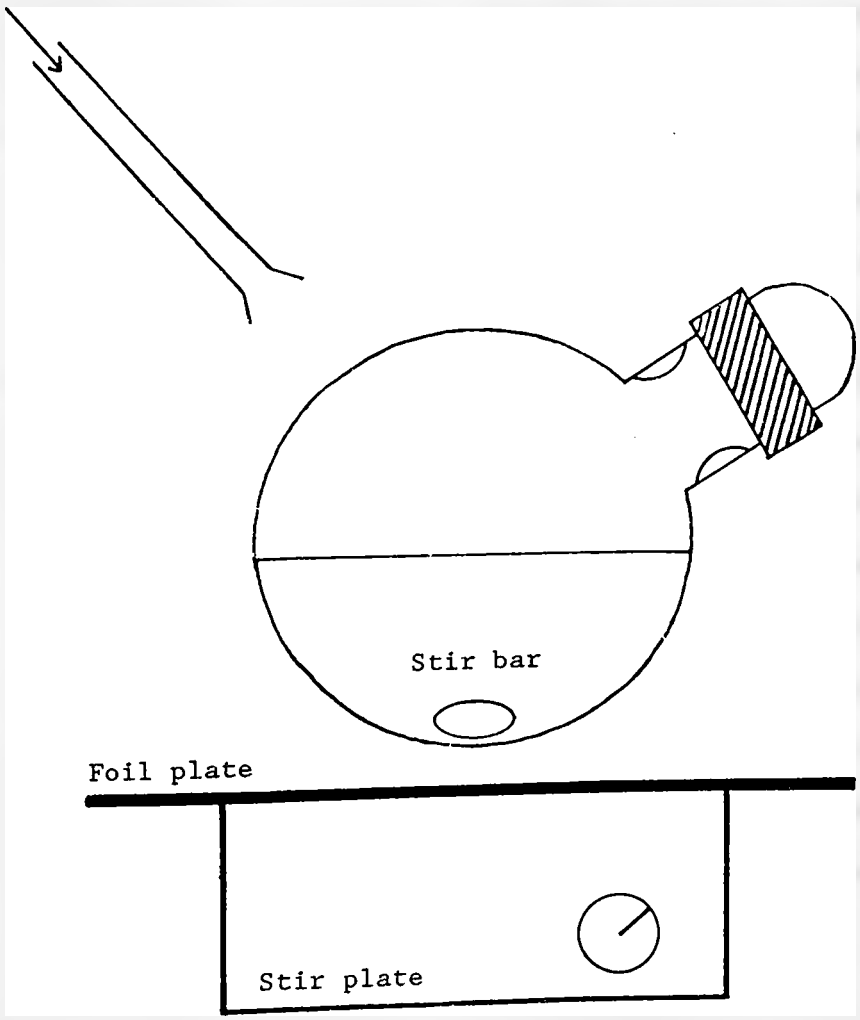

or C_5), 49.84(C_8), 50.37(C_{12}), 126.44, 127.01, 129.29(C_{15}-C_{20}), 161.74, 176.60(C_1,C_2,C_6 and C_7). Elemental analysis: calculated 44.1% C, 5.5% H, 10.3% N; found 43.90% C, 5.46% H, 9.57% N. Mass spectrum: m/e (relative intensity) 544(0.43), 528(0.40), 453(0.37), 91(100).

2,2,6,6-tetramethyl-1-benzyloxy-piperidine, benzylTEMPO, was prepared by the combined methods of Smith[19], Waddington[20], and Martin[21]. A 250 ml 1-neck round bottom flask equipped with a pressure-releasing addition funnel was taken through three cycles of vacuum purging and back-filling with N_2. Next 20 mls (40 mmol) of 2.0 M Benzyl Magnesium Bromide in THF (Aldrich) were added, followed by 20 mls of degassed ether. In a separate flask, 14.58 g (93 mmol) of TEMPO were dissolved in 20 mls of degassed ether. The TEMPO solution was transferred by needlestock to the addition funnel. The Grignard solution was cooled to -10°C with a salt water bath and the TEMPO solution was added dropwise over 1 hour while the mixture was stirred by magnetic stir bar until the orange color indicating excess TEMPO persisted. The mixture was a cloudy orange, the cloudiness due to insoluble $MgBr_2$. The mixture was exposed to the atmosphere and 20.3 g of NH_4Cl in 100 mls of distilled water were added. The precipitate dissolved and the solution turned dark orange. Two immiscible layers became visible. The solution was allowed to warm to room temperature and was placed in a 250 ml separatory funnel. The aqueous layer was removed and the organic layer washed with distilled water (125 mls, 2 times). The organic solution was then transferred to a 150 ml erlehnmeyer flask and dried overnight with $MgSO_4$. The next day, the solution was placed first under vacuum aspirator and then high vacuum to remove the volatile solvents, ether

and THF. The desired product was purified to approximately 90% by NMR using preparative gas chromatography (column conditions: 1.5% OV-101, 100/120, injector 185°C, detector 225°C, column 130-200°C). A total of six peaks were seen by G.C. and were determined to be ether, toluene, THF, TEMPO, bibenzyl, and benzylTEMPO in that order. Benzyl-TEMPO was the largest peak and made up approximately 60-70% of the total crude mixture. The total yield of the preparation was not determined as only enough product as was needed for further experiments was collected (ca. 500 mg). Ideally, it would have been best to have a sample of pure benzyl-TEMPO as it was used to quantify the amount produced in the 2 + TEMPO thermolysis reaction. However, even upon three-fold preparative G.C. purification of a sample of benzylTEMPO, a small amount of TEMPO and bibenzyl are found. These are the decomposition products of benzylTEMPO. Adjusting the column temperatures did not help as, at lower temperatures, the bibenzyl and benzylTEMPO peaks begin to broaden and blend together. This problem was side-stepped simply by quantifying the amount of bibenzyl, TEMPO, and benzyl-TEMPO in the purified mixture by analytical gas chromatrography. ^{1}H NMR (acetonitrile-d_3) δ 1.1-1.5(m,18H), 4.78(s,2H), 7.36(m,5H) (in agreement with literature values).[22]

Product Studies

X-ray Structural Analysis of 2

Black lath-shaped crystals were grown from an oxygen-free benzene solution of 2, washed with hexane, and sucked dry on a glass frit in a glove-box, then sealed in Lindemann glass capillaries. Intensity data were obtained from one crystal at Molecular Structures Corporation, College Station, TX, after cell dimensions had been calculated from the setting angles of 23 centered reflections in the range $20.1 \leq 2\theta \leq 24.1^{o}$. Crystal parameters and particulars of data collection and refinement are given in Appendix 2, Table A1. Because the crystal diffracted weakly, only 51% of the independent reflections scanned were observed, but no problems were experienced during the structure analysis. The *TEXSAN* program suite[23], installed on a MicroVAX II/RC computer at Oregon State University, was used in all calculations. The distribution of intensities was clearly centric. The approximate positions of the iodine and cobalt atoms were obtained from a Patterson synthesis. All other non-hydrogen atoms, including the three independent carbon atoms of a molecule of benzene solvate, were located from a single cycle of *DIRDIF*.[24] All non-hydrogen atoms other than the benzene atoms C(21,22,23) were allowed anisotropic thermal parameters in the later cycles of full-matrix least-squares refinement, and hydrogen atoms were included at calculated positions with B values constrained to 1.2 times the values of B_{eq} for the parent atoms. The maximum deviation from planarity in the final difference synthesis was +0.90 e $Å^{-3}$, *ca.* 1.0 Å

from the iodine atom. Scattering factors were taken from refs. 25 (H) and 26 (other atoms).

Photolysis of 1 at UV/Vis. Concentration

30 mg (0.055 mmol) of 1 were dissolved in 10 mls of benzene. 200 mls of this solution were diluted to 10 mls with benzene. Final [1] = 1.1×10^{-4} M. A UV/vis cuvette was filled with this solution, covered with foil, and brought out of the box. The cuvette was photolysed with a GE sunlamp at 30 cm, while lying on a reflective foil plate. The reaction was followed periodically by visible spectroscopy.

2 + TEMPO Thermolysis/ G.C. Product Analysis

3.3 mg of 2 were dissolved in 0.60 mls of d_6-benzene in an airtight NMR tube in the box. 32 mg (34 eq.) of TEMPO were added to the tube. The tube was sealed, removed from the box, and thermolysed for ca. 28 hrs. in a 69°C oil bath. The tube was removed from the bath and taken back into the box where 1.4 ml of heptane were added. The solution was transferred to a 3 ml vial, capped with a septum, and removed from the box for G.C. analysis.

500Mhz NMR of 2

In the drybox, 47 mg of 2 were dissolved in 2 mls of deuterobenzene. The solution was filtered through glass wool into an airtight NMR tube an sealed. The tube was brought out of the box and

submitted to Chuck Klopfenstein for a 500 MHz NMR to examine the hydroxylic proton of 2 that appears at δ 17.47 and an unidentified peak that appears at δ 17.37.

NMR Analysis of 2 in Protic Solvents

Crystals of 2 (ca. 2 mg) were dissolved on 0.50 mls of d_6-acetone in an airtight NMR tube in the drybox. The tube was sealed, removed from the box, and an NMR was taken. The acetone was removed under vacuum, and the precipitate was redissolved in d_4-methanol in the box. Again, the tube was sealed, removed from the box, and an NMR was taken. 2-4 mg of crystals of 2 were dissolved in 0.60mls of $CDCl_3$ in an airtight NMR tube in the box. The tube was sealed, removed from the box and an NMR was taken.

Equilibrium and Kinetic Studies

Short T_1 Relaxation Experiment

A few mg of 1 were dissolved in 1 ml of deuterated benzene in an airtight NMR tube (the solution was less than saturated). The tube was thermolysed at 70°C for ca. 3 hrs to produce some 2. The reaction was quenched and three NMRs were taken. A relaxation time of 1 sec was used and the magnet was shimmed between each NMR. The two downfield protons of 1 and 2 were integrated versus TMS internal standard and the fraction of 1 was calculated. Three more NMRs were taken, this time with a longer relaxation time of 10 sec, and again the magnet was shimmed

between each NMR. Again the two downfield protons were integrated and the fraction of 1 was calculated.

Thermolysis of 1 at NMR Concentration with Ph_3CH

Triphenylmethane (TPM) was chosen as the internal standard because it has a singlet at δ 5.140, where no other peaks (1 or 2) show up. In addition it is quite stable and does not interfere with the reaction. 9.67 mg (0.0178 mmol) of 1 and 2.45 mg (0.0100 mmol) of TPM were dissolved in 1.25 mls of deuterated benzene in an airtight NMR tube. [1] = 1.42×10^{-2} M. [TPM] = 8.02×10^{-3} M. The tube was thermolysed at 69.0 ± 0.2°C and the reaction was followed by NMR.

Thermolysis of 2 at NMR Concentration with Ph_3CH

The tube from the above reaction was photolysed to pure 2 (clean NMR with good resolution). The tube was then thermolysed at 69.0 ± 0.2°C and the reaction followed by NMR.

UV/vis Evaluation of 1 Thermolysis at NMR Concentration

In order to help prove that Co^{II} is not formed in the thermolysis reaction, a UV/vis spectrum of the equilibrium mixture is necessary. 4.89 mg (0.00898 mmol) of 1 were dissolved in 1.25 mls of deuterated benzene. No internal standard was used for it could interfere with the UV/visible spectrum. [1] = 7.19×10^{-3} M. The tube was thermolysed as before at 69.0 ± 0.2°C for ca. 42 hrs. Subsequent NMR showed that the

reaction had reached equilibrium (39% 1 by integration). The tube was taken into the box and a few drops of the reaction mixture were placed in a UV/vis cuvette with benzene. This was all done with protection from light to prevent the reaction from continuing further. The cuvette and NMR tube were both sealed and a visible spectrum of the cuvette was taken. The NMR tube was then photolysed until the reaction was complete. The tube was taken back into the box and another cuvette of the reaction mixture was made up. A visible spectrum of this cuvette was taken as well.

Thermolysis of 1 and 2 at UV/vis Concentrations

In the drybox 6.3 mg of 1 were dissolved in 10.0 mls of benzene. 0.3 mls of this solution were diluted to 3.0 mls ([1] = 1.2×10^{-4} M). This solution was placed in an air-tight cuvette, brought out of the box, and thermolysed in the dark at 69.0 ± 0.2°C for 462 minutes. The reaction was followed to completion (no change in consecutive spectra) by visible spectroscopy. The cuvette was then photolysed for 40 minutes and monitored by visible spectroscopy until the reaction was complete. Finally, the cuvette was again thermolysed at 69.0°C for 1755 minutes until the reaction was complete.

Simultaneous Photolysis/thermolysis of 1 at UV/vis Concentrations

In the drybox 5.0 mg of 1 were dissolved in 10.0 mls of benzene. 0.3 mls of this solution were diluted to 3.0 mls ([1] = 9.2×10^{-5} M). This solution was placed in an airtight cuvette, brought out of the box,

and photolysed while submerged in an oil bath at 69.0 ± 0.2°C. The reaction was followed by visible spectroscopy for 69 minutes to completion.

85°C Thermolysis of 1 at NMR Concentration

In the drybox ca. 5 mg of 1 were dissolved in 1ml of deuterated benzene in an air-tight NMR tube. The tube was removed from the box and thermolysed for ca. 36 hours at 69.2 ± 0.2°C to produce the known 1/2 equilibrium mixture. The tube was then thermolysed for an additional 48 hours at 85 ± 2°C. At the end of this time, the tube was quenched and NMRs were taken.

Thermolysis of 2 with TEMPO

33 mg (0.061 mmol) of 2 was dissolved in 10 mls of benzene, then 0.30 mls of this solution was diluted to 10.0 mls with benzene and 3.25 mls of this solution were placed in a sidearm-equipped UV/vis cuvette. Next, 0.25 mls of 3.20×10^{-2} M TEMPO was added to the sidearm. The cuvette was capped, taken out of the box, the TEMPO and 2 were mixed just prior to taking the first visible spectrum, and the time was noted. [2] = 1.7×10^{-4} M. [TEMPO] = 2.3×10^{-3} M (14 eq). The cuvette was thermolysed at 60 ± 0.2°C and again, the reaction was followed periodically by visible spectra. Three more cuvettes were made up in the same fashion and were thermolysed at 70° 75° and 90°C. These reactions were also followed by visible spectroscopy as prescribed above.

APPENDICES

Appendix 1: Calculations for kinetic and equilibrium experiments at 69°C

1) $K_{eq69°C} = 1.5 \pm 0.1 = k_1/k_{-1}$

2) $k_{obs} = (3.6 \pm 0.7) \times 10^{-5}\ sec^{-1}M^{-1} = k_1 + k_{-1}$

3) $k_1 = (2.2 \pm 0.9) \times 10^{-5}\ sec^{-1}M^{-1}$

4) $k_{-1} = (1.4 \pm 0.3) \times 10^{-5}\ sec^{-1}M^{-1}$

5) $\Delta G = -RT\ln K_{eq} = -0.28 \pm 0.02$ kcal/mol $= \Delta H - T\Delta S$

Because K_{eq} is temperature independent within 2%, ΔH is equal to 0 ± 0.2 kcal; that is, the driving force behind the equilibrium is ΔS within experimental error.

Given: $\Delta H = 0 \pm 0.2$ kcal

Then: $\Delta S = -\Delta G/T = 0.82 \pm 0.06$ cal/mol•K

Appendix 2: Supplementary material to the crystal structure of 1:

Table A1: X-ray structural analysis

Crystal data:	
formula	$C_{20}H_{30}CoIN_4O_2 \cdot 0.5C_6H_6$
system, space-group	triclinic, P1
a, b, c (Å)	9.966(1), 16.514(3), 7.892(3)
α, β, ρ	101.42(2), 90.66(2), 77.70(1)
V (Å^3)	1243(1)
Z	2
D_{calc} (g cm^{-3})	1.56
μ (cm^{-1})	20.0
F_{000}	594
Intensity measurement:	
crystal appearance	black lath
crystal size (mm)	0.30 x 0.15 x 0.07
diffractometer	Rigaku AFC6R
radiation, λ (Å)	Mo Kα, 0.71069
monochromator	graphite
transmission factors	0.84-1.00
absorption correction	ψ-scan
scan mode	ω-2θ
scan width (deg)	0.84 + 0.30tanθ
scan speed in l (deg min^{-1})	16
$2r_{max}$	50.2
octants	+h,±k,±l

T (^{o}C)	23
number of rflns scanned (total)	4702
number of rflns (independent)	4422
standard rflns	3, every 150 (no change)
R_{int}, ±(0kl)	0.010
Refinement (on F):	
number of observed data	2258 [I≥3s(I)]
number of parameters	265
function minimized	$Rw(\|F_o\|-\|F_c\|)^2$
weighting factor	$\sigma^{-2}(F)$
R, wR	0.052, 0.061
goodness-of-fit index	1.29
max. Δ/σ, last cycle	0.03

Table A2: Atomic coordinates (x 10^4) and equivalent isotropic thermal parameters (Å^2)

Atom	x	y	z	B_{eq}
I(1)	2991.9(8)	3283.8(5)	4020(1)	4.38(4)
Co(1)	5377(1)	2324.7(8)	4790(2)	2.91(7)
O(1)	5614(8)	1181(4)	1510(8)	4.2(4)
O(2)	7327(8)	2074(5)	2191(9)	4.6(4)
N(1)	5136(8)	1373(5)	3205(10)	3.0(4)
N(2)	4379(8)	1814(5)	6227(10)	3.0(4)

N(3)	5806(9)	3190(5)	6555(11)	3.6(5)
N(4)	6830(8)	2469(5)	3684(11)	3.4(5)
C(1)	4305(10)	922(6)	3610(13)	2.9(5)
C(2)	3902(10)	1187(6)	5404(13)	2.9(5)
C(3)	4033(12)	2156(7)	8066(13)	4.0(6)
C(4)	4966(12)	2699(7)	8947(13)	4.0(6)
C(5)	5020(12)	3457(6)	8189(13)	4.1(6)
C(6)	6803(11)	3522(7)	6230(14)	3.5(6)
C(7)	7578(11)	3121(7)	4543(14)	3.7(6)
C(8)	3636(12)	261(7)	2309(13)	3.9(6)
C(9)	2607(14)	663(8)	1395916)	5.5(8)
C(10)	2887(12)	793(7)	6193(16)	4.7(7)
C(11)	7244(13)	4244(8)	7377(17)	5.6(8)
C(12)	7641(13)	3761(7)	3373(15)	4.8(7)
C(13)	6258(14)	4238(7)	2927(16)	5.1(7)
C(14)	9070(11)	2673(7)	4836(15)	4.3(6)
C(15)	9235(11)	2130(7)	6167(15)	3.9(6)
C(16)	9010(11)	1324(9)	5780(17)	5.1(7)
C(17)	9150(14)	818(9)	6969(25)	6.5(9)
C(18)	9482(16)	1133(12)	8621(24)	7.2(10)
C(19)	9721(15)	1929(11)	9085(17)	6.7(9)
C(20)	9601(14)	2420(8)	7820(19)	5.5(8)
C(21)	161(14)	4647(8)	1464(17)	5.8(3)
C(22)	1022(14)	4324(8)	46(18)	6.1(3)
C(23)	847(14)	4654(8)	8620(17)	6.0(3)

The equivalent isotropic thermal parameter is defined by:

$$B_{eq} = (8p^2/3)\Sigma_i\Sigma_j U_{ij} a^*_i a^*_j a_i \cdot a_j$$

Table A3: Bond lengths (Å) and interbond angles (deg)

I(1)-Co(1)	2.697(2)	C(4)-C(5)	1.501(14)
Co(1)-N(1)	1.862(7)	C(6)-C(7)	1.505(13)
Co(1)-N(2)	1.936(8)	C(6)-C(11)	1.492(14)
Co(1)-N(3)	1.904(7)	C(7)-C(12)	1.546(15)
Co(1)-N(4)	1.781(7)	C(7)-C(14)	1.550(14)
O(1)-N(1)	1.378(10)	C(8)-C(9)	1.511(15)
O(2)-N(4)	1.277(10)	C(12)-C(13)	1.511(15)
N(1)-C(1)	1.306(12)	C(14)-C(15)	1.497(13)
N(2)-C(2)	1.288(13)	C(15)-C(16)	1.371(12)
N(2)-C(3)	1.466(13)	C(15)-C(20)	1.371(15)
N(3)-C(5)	1.457(13)	C(16)-C(17)	1.353(13)
N(3)-C(6)	1.282(12)	C(17)-C(18)	1.370(15)
N(4)-C(7)	1.489(13)	C(18)-C(19)	1.363(15)
C(1)-C(2)	1.432(15)	C(19)-C(20)	1.395(13)
C(1)-C(8)	1.492(15)	C(21)-C(22)	1.366(13)
C(2)-C(10)	1.514(14)	C(21)-C(23)	1.371(13)
C(3)-C(4)	1.499(13)	C(22)-C(23)	1.339(13)
O(1)...O(2)	2.473(9)		
I(1)-Co(1)-N(1)	93.1(2)	C(1)-C(2)-C(10)	120.9(9)
I(1)-Co(1)-N(2)	90.0(2)	N(2)-C(3)-C(4)	114.0(9)

I(1)-Co(1)-N(3)	94.5(2)	C(3)-C(4)-C(5)	115.1(10)
I(1)-Co(1)-N(4)	113.0(2)	N(3)-C(5)-C(4)	109.8(9)
N(1)-Co(1)-N(2)	79.5(3)	N(3)-C(6)-C(7)	115.3(9)
N(1)-Co(1)-N(3)	172.0(3)	N(3)-C(6)-C(11)	125.7(9)
N(1)-Co(1)-N(4)	95.6(3)	C(7)-C(6)-C(11)	119.0(10)
N(2)-Co(1)-N(3)	97.9(3)	N(4)-C(7)-C(6)	105.2(9)
N(2)-Co(1)-N(4)	156.8(3)	N(4)-C(7)-C(12)	110.4(9)
N(3)-Co(1)-N(4)	83.8(3)	N(4)-C(7)-C(14)	108.4(9)
Co(1)-N(1)-O(1)	123.6(6)	C(6)-C(7)-C(12)	113.0(10)
Co(1)-N(1)-C(1)	119.3(6)	C(6)-C(7)-C(14)	111.5(11)
O(1)-N(1)-C(1)	116.3(7)	C(12)-C(7)-C(14)	108.1(12)
Co(1)-N(2)-C(2)	114.6(6)	C(1)-C(8)-C(9)	109.9(13)
Co(1)-N(2)-C(3)	124.1(6)	C(7)-C(12)-C(13)	114.7(13)
C(2)-N(2)-C(3)	120.9(9)	C(7)-C(14)-C(15)	116.0(12)
Co(1)-N(3)-C(5)	120.6(6)	C(14)-C(15)-C(16)	121.0(13)
Co(1)-N(3)-C(6)	117.0(6)	C(14)-C(15)-C(20)	121.5(13)
C(5)-N(3)-C(6)	122.4(9)	C(16)-C(15)-C(20)	117.5(13)
Co(1)-N(4)-O(2)	127.5(6)	C(15)-C(16)-C(17)	122.2(13)
Co(1)-N(4)-C(7)	118.5(6)	C(16)-C(17)-C(18)	118.9(14)
O(2)-N(4)-C(7)	114.1(70	C(17)-C(18)-C(19)	121.6(15)
N(1)-C(1)-C(2)	110.1(9)	C(18)-C(19)-C(20)	117.7(4)
N(1)-C(1)-C(8)	122.5(9)	C(15)-C(20)-C(19)	122.0(13)
C(2)-C(1)-C(8)	127.3(9)	C(22)-C(21)-C(23)	116.7(14)
N(2)-C(2)-C(1)	115.2(9)	C(21)-C(22)-C(23)	121.3(14)
N(2)-C(2)-C(10)	123.7(9)	C(22)-C(23)-C(21)	121.9(13)

Supplementary material

Table S1: Calculated coordinates (x 10^4) and thermal parameters ($Å^2$) for hydrogen atoms in last cycle of refinement.

Atom	x	y	z	B
H(1)	3121	2486	8167	4.8
H(2)	4080	1695	8635	4.8
H(3)	4663	2893	123	4.8
H(4)	5869	2360	8889	4.8
H(5)	5447	3833	8972	4.9
H(6)	4112	3738	7994	4.9
H(7)	4560	-11	1485	4.7
H(8)	3588	-144	2878	4.7
H(9)	1884	940	2219	6.6
H(10)	2856	1064	814	6.6
H(11)	2307	238	578	6.6
H(12)	2072	1208	6556	5.7
H(13)	2672	343	5357	5.7
H(14)	3279	579	7162	5.7
H(15)	7512	4095	8453	6.7
H(16)	7999	4374	6842	6.7
H(17)	6503	4724	7567	6.7
H(18)	8136	4161	3952	5.8
H(19)	8119	3461	2325	5.8
H(20)	5774	4557	3958	6.2
H(21)	6384	4610	2193	6.2
H(22)	5744	3848	2350	6.2

H(23)	9436	2324	3766	5.2
H(24)	9585	3096	5180	5.2
H(25)	8747	1112	4646	6.1
H(26)	9020	254	6657	7.8
H(27)	9547	790	9464	8.6
H(28)	9962	2141	230	8.0
H(29)	9779	2973	8112	6.6
H(30)	255	4399	2460	7.0
H(31)	1761	3856	71	7.3
H(32)	1438	4397	7638	7.1

Table S2: Anisotropic thermal parameters (x 10^3) ($Å^2$)

Atom	U_{11}	U_{22}	U_{33}	U_{12}	U_{13}	U_{23}
I(1)	45.3(5)	59.3(5)	60.3(6)	-1.9(4)	3.2(4)	7.8(4)
Co(1)	35.0(9)	39.0(8)	36.1(8)	-9.1(7)	7.2(7)	5.1(6)
O(1)	63(5)	64(5)	32(4)	-23(4)	16(4)	5(3)
O(2)	49(5)	80(6)	42(5)	-17(4)	23(4)	2(4)
N(1)	32(5)	42(5)	39(5)	-14(4)	3(4)	4(4)
N(2)	32(5)	43(5)	36(5)	-1(4)	11(4)	10(4)
N(3)	43(5)	48(5)	46(6)	-12(4)	6(4)	9(4)
N(4)	41(5)	53(5)	41(5)	-23(4)	7(4)	8(4)
C(1)	31(6)	26(5)	48(7)	1(5)	-1(5)	5(5)
C(2)	30(6)	42(6)	44(6)	-12(5)	20(6)	11(5)
C(3)	60(8)	56(7)	40(7)	-15(6)	20(6)	11(5)
C(4)	69(8)	48(7)	36(6)	-12(6)	6(6)	7(5)

C(5)	67(8)	46(7)	36(6)	-7(5)	0(6)	-4(5)
C(6)	43(7)	45(6)	47(7)	-7(5)	-5(5)	16(5)
C(7)	33(6)	55(7)	57(7)	-19(5)	6(5)	11(6)
C(8)	55(7)	57(7)	43(7)	-28(6)	12(6)	5(5)
C(9)	80(10)	80(10)	63(8)	-36(8)	-24(7)	26(7)
C(10)	50(7)	57(8)	81(10)	-22(6)	8(7)	22(7)

The temperature factor is given by:

$$T = \exp[-2\pi^2 \Sigma_i \Sigma_j U_{ij} h_i h_j a_i^* a_j^*]$$

Appendix 3: Gas chromatography (G.C.) calculations.

Calibration:

The yield of benzyl-TEMPO was quantified using an HP5790 gas chromatograph, flame ionization detection (225°C, H_2 combustion, N_2 carrier gas), and 50:1 nominal split-flow capillary injection system (150°C). The column oven program was 125°C for 2.5 min, increasing at 10°C/min for 3.5 min to 160°C. The non-default HP3390A integrator settings were att. = -1, thresh. = -1.

Quantification:

compound	temp	retention time
Heptane	125°C	1.98 min
Benzene	125°C	2.19 min
TEMPO[a]	125-160°C gradient	4.5-5.5 min
Bibenzyl[b]	160°C	19.69 min
BenzylTEMPO[c]	160°C	18.89 min

[a] Std. TEMPO solution: 0.20 M TEMPO, 1.1 M Heptane in Benzene → 4 injections gave $F_T = 1.15 \pm 0.09$ from eq. 1

[b] Std. Bibenzyl solution: 0.16 M Bibenzyl, 0.62 M Heptane in Benzene → 3 injections gave $F_{BB} = 1.18 \pm 0.09$ from eq. 1

[c] Six injection of ca. 0.2 M BenzylTEMPO (purified by prep G.C.) gave as average percentages:

90.4 ± 0.5% BenzylTEMPO

7.0 ± 0.2% Bibenzyl

2.7 ± 0.5% TEMPO

Std. BenzylTEMPO solution: 3.6×10^{-2} M BenzylTEMPO (based on 90.4% purity), 6.7×10^{-2} M Heptane in Benzene → 3 injections gave F_{BT} = 0.99 ± 0.2 from eq. 1

eq. 1 $[X]/[std] = (\text{area } X/\text{area std})F_X$

[2] = 1.0×10^{-2} M

[TEMPO] = 3.4×10^{-2} M

[Heptane] = 1.6×10^{-2} M

Theoretical [BenzylTEMPO] = 1.0×10^{-2} M

[BenzylTEMPO] = (area BenzylTEMPO/area Heptane)[Heptane]F_{BT}

3 injections gave mean area (BenzylTEMPO/area Heptane) = 0.60 ± 2%

[BenzylTEMPO] = (0.60 ± 2%)(6.7×10^{-2} M)(0.99 ± 2%)

= 9.5×10^{-3} M ± 6% (including 5% G.C. error)

% yield = 9.5×10^{-3} M/1.0×10^{-2} M

= 95 ± 6% BenzylTEMPO

GLOSSARY

Axial - pertaining to those molecules attached to cobalt but lying in the plane perpendicular to the equatorial corrin ligand in the case of B_{12}.

Corrin Ring - the part of B_{12} in the equatorial plane made up of the four nitrogens surrounding it.

Elemental Analysis is used to determine purity of a sample. The theoretical weight percent of each atom in a molecule can be calculated by multiplying the molecular weight of the particular atom by the number of atoms of this type that are in the molecule; one then divides the resultant number by the molecular weight of the entire molecule. The sample is then combusted and the actual weight percent is determined. The experimental and theoretical values are compared to evaluate purity (identical $\pm$ 0.4% for pure compounds).

Enantiomers - Optical isomers that are not superimposable mirror images of one another.

Equatorial ligand - the corrin ring in the case of B_{12} (ie. the molecule which lies in the equatorial plane of a six coordinate metal atom).

Free radical trap - a molecule with an unpaired electron which irreversibly bonds to free radicals, thereby "trapping" them.

Homolysis - the breaking of a molecular bond by heat, light, or other energy input in which one of the two electrons in the bond goes to each of the two atoms being separated by the breakage. The result is no net charge on either of the fragments which both now have an unpaired

electron. These fragments are known as free radicals (ie. freely diffusing radicals).

Isomers - Two or more molecules having the same number and type of atoms, that is compounds with the same molecular formula.

Isosbestic point - if two substances of equal concentrations have absorption bands that overlap, there will be some wavelength at which the molar absorbtivities of the species are equal. If the sum of the concentrations of these two materials in solution is held constant, there will be no change in absorbance at this wavelength as the ratio of the two materials is varied. This invariant point is referred to as the isosbestic point. The presence of this point during a chemical reaction is thus good evidence for the presence of only two species and that no others are building up. It is possible, however, to have, in some special instances, three or four species present and still have an isosbestic point if the concentrations of all the species are related by an equilibrium expression.

Mass Spectroscopy is used to determine the molecular weight, connectivity, and structure of a molecule. The sample is bombarded with energetic electrons (conventional e- impact mass spectroscopy) or atoms (fast atom bombardment mass spectroscopy) at high velocity which fragments the molecule in any variety of ways. A spectrum of fragments as a function of molecular weight is generated, and this spectrum is used to determine the total molecular weight of the molecule and the molecular weights of the various fragments. Because the molecule does not fragment the same way every time and weaker bonds will fragment more frequently than stronger bonds, the, by looking at the combined data of fragment size and frequency of occurrence of a particular fragment, one

can gain information about structure, continuity, and even relative stability (compared to other similar molecules) of a molecule.

Optical isomers - Isomers that differ from each other only in the direction in which they rotate plane-polarized light.

Photolysis - exposure to light induce a homolysis reaction (ie. photochemical homolysis).

Spectroscopy - Organic or organometallic products of chemical reactions are analyzed primarily through the use of spectroscopic techniques including: Nuclear Magnetic Resonance (NMR) and Ultraviolet/visible spectroscopy (UV/Visible). The key to spectroscopy is that no two different of molecules have the same spectrum, except in some unusual cases. NMR looks at the hydrogen atoms in a molecule. The sample is placed in a magnetic field of varying frequency and the hydrogen atoms are excited and relaxed and the signal is converted into a spectrum. Peaks representing the various hydrogen atoms are plotted versus frequency. Depending on their position in the molecule, different hydrogen atoms are excited at different frequencies of electromagnetic radiation. By integrating the peaks and determining their area, the relative number of each type of hydrogen atom in the molecule can be determined. This provides valuable information about the molecule's structure - essentially, it allows the chemist too count the number and different types of hydrogens in a molecule. By watching the appearance or disappearance of a particular peak as a function of time, the rate of reaction can be determined.

UV/Visible spectroscopy looks at the absorption of UV and/or visible light by a molecule. Light of varying wavelength, but in the UV/visible region, is passed through a dilute solution of the compound

and detected on the other side. A given molecule will absorb more light at some wavelengths than at others. Absorbance is plotted as a function of wavelength and a characteristic spectrum is generated. By watching a maximum absorbance disappear with time or a minimum grow in with time, a rate of reaction can be determined.

Both the NMR and UV/Visible spectra of 1 and the rearrangement product have been determined. Thus, the spectra from my experiments will be compared with the expected spectra, or those of closely similar molecules to evaluate composition and purity.

Structural isomer - isomers which have different atoms and/or bonding patterns in relation to each other.

Tautomers - isomers that differ only in the position of a proton (usually) within the molecule. There exists a rapid shift of the proton back and forth between atoms within the molecule.

Thermolysis - heating in the absence of light to induce a homolysis reaction (ie. thermal homolysis).

X-ray Crystallography is used to determine the precise three-dimensional structure of a molecule. It is the single most powerful technique available in chemistry and biochemistry to determine a molecule's exact structure. It is limited only by the availability of good crystals and the so-called phasing problem. Crystals of a molecule are grown and mounted and x-rays are directed at the crystals. The crystals diffract the x-rays and the diffraction pattern is recorded on film. Every type of molecule gives a unique diffraction pattern. The diffraction pattern is analyzed by computer and from this data a three-dimensional structure is generated. The only other limitation of this powerful method is that it is applicable only to crystals, that is, to the solid state. Large

molecules (ie. enzymes) can have many different structures (ie. orientations) in solution, only one of which may (or may not) be the solid state structure.

REFERENCES

[1]Finke, R.G., Smith, B.L., Mayer, B.J., Molinero, A.A. *Inorg. Chem.* 1983, *22*, 3677-3679.

[2]Le Hoang, M. D.; Robin, Y.; Deuynch, J.; Beid-Charreton, C.; Gaudemer, A.; *J. Organomet. Chem.* 1981, *222*, 311-321

[3]Balch, A.L., Latos-Grazynski, L., Cheng, R., LaMar, G. J. Am. Chem. *Soc.* 1981, *103*, 4270-4272.

[4]Mansuay, D., Battioni, J., Dupre, D., Sartori, E. *J. Am. Chem.Soc* 1982, *104*, 6159-6161.

[5]Mansuy, D.; Battioni, J.; Dupre', D.; Sartori, E.; Chottard, G.; *J. Am. Chem. Soc.*, 1982, *104*, 6159-6161.

[6]Mansuy, D.; Battioni, J.; Akhrem, I.; Dupre', D.; Fischer, J.; Weiss, R.; Morgenstern-Baradou, I.; *J. Am. Chem. Soc.*, 1984, *106*, 6112-6114.

[7]McHatten, R.; Espenson, J.; Bakac, A.; *J. Am. Chem. Soc.*, 1986, *108*, 5885-5890.

[8]Samsel, E. G.; Kochi, J. K.; *J. Am. Chem. Soc.*, 1986, *108*, 4790-4804.

[9]Finke, R.G.; *Personal Communication*, August 1988.

[10]Weakley. T.J.R.; *Report on the Crystal Structural Analysis of* 1, 1989.

[11]Fischer, Hans; *J. Am. Chem. Soc.*, 1986, *108*, 3925-3927.

[12]Galamb, V.; Palyi, G.' Ungva'ry, F.; Marko, L.; Boese, R.; Schmid, G.; *J. Am. Chem. Soc.*, 1986, *108*, 3344-3351.

[13]Koenig, T.W.; Hay B.P.; Finke, R.G.; *Polyhedron*, 1988, 7, 1499.

[14]McMillan, D.F.; Golden, D.M.; *Ann. Rev. Phys. Chem.*, 1982, *33*, 493-532.

[15]Finke, R.G.; Coenzyme B_{12}-Dependent Rearrangement Reactions: Chemical Precedent for Ke Elementary Steps and Insight into Enzyme-Assisted Cobalt-Carbon Bond Cleavage. Presented to the Royal Society of Chemistry Joint Perkin Division-Bioorganic Group Meeting, International Symposium on Molecular Mechanisms in Bioorganic Processes. July 17-20, 1989, University of Newcastle Upon Tyne, England.

[16]Gray, N.E. *Research Report #1*. Finke Group, U of O, 1987

[17]Aldrich Handbook of Fine Chemicals, 1986-1987, 1218.

[18]Finke, R.G., Smith, B.L., McKenna, W.A., Christian, P.A. *Inorg. Chem.* 1981, *20*, 687-693.

[19]Smith, B. L.; *Ph.D. Dissertation,* University of Oregon, 1982, 167.

[20]Finke, R. G.; Waddington, M. D.; *Manuscript in Progress*.

[21]Martin, B. D.; *Research Report #1*, Finke group, University of Oregon, 1988, 39.

[22]Johnston, Linda J.; Tencer, Michal; Scaiano, J.C.; *J. Org. Chem.*, 1986, 51 2806-2808.

[23]*TEXSAN Texray Structural Analysis program suite,* Molecular Structures Corporation, College Station, TX, 1987.

[24]Buerskens, P.T. *DIRDIF: Direct Methods for Difference Structures*, Technical Report 1984/1, Crystallographic.

[25]Stewart, R.F.; Davidson, E.R.; Simpson, W.T. *J. Chem. Phys.*, 1965, 42, 3175-3187.

[26]Cromer, D.T.; Waber, J.T. In *International Tables for X-ray Crystallography*, Kynoch Press, Birmingham, England, 1974, vol. I, pp. 71, 148.